A Game Theoretic Approach to Uplink Pilot and Data Power Control in Multi-Cell Multi-User MIMO Systems

Peiyue Zhao, Gábor Fodor, György Dán, Miklós Telek

Abstract—In multi-user multiple input multiple output (MU-MIMO) systems that employ pilot-symbol aided channel estimation, the pilot-to-data power ratio (PDPR) has a large impact on the system performance. In this paper we consider the problem of setting the PDPR in multi-cell MU-MIMO systems in the presence of channel estimation errors, intercell interference and pilot contamination. To analyze and address this problem, we first develop a model of the multi-cell MU-MIMO system and derive a closed-form expression for the mean squared error of the uplink received data symbols. Building on this result, we then propose two decentralized PDPR-setting algorithms based on game theoretic approaches that are applicable in multi-cell systems. We find that both algorithms converge to a Nash equilibrium and provide performance improvements over systems that do not properly set the PDPR, while they maintain different levels of fairness.

Keywords: multi-antenna systems, channel state information, estimation techniques, receiver algorithms

I. INTRODUCTION

In the uplink of multi-user multiple input multiple output (MU-MIMO) systems, the base station (BS) typically acquires channel state information (CSI) by means of uplink pilot or reference signals that are orthogonal in the code domain. long term evolution (LTE) systems, for example, use the cyclically shifted Zadoff-Chu sequences to acquire CSI at the receiver for uplink data reception [1]. It has been pointed out by several related works that in systems employing pilot aided channel estimation, the pilot-to-data power ratio (PDPR) plays a crucial role in optimizing the inherent trade-off between sharing the available resources between pilot and data symbols [2]–[5].

The seminal work by [2] established lower and upper bounds on the difference between the mutual information when the receiver has only an estimate of the channel and when it has perfect knowledge of the channel. Subsequently, the results in [3] showed how training-based channel estimation affects the capacity of the fading channel, recognizing that training imposes a substantial information-theoretic penalty, especially when the coherence interval T (measured in terms of the number of symbols available for pilot and data transmission) is only slightly larger than the number of transmit antennas M, or when the SNR is low. Subsequently, the authors in [4] and [6] established a lower bound specifically for MIMO orthogonal frequency division multiplexing (OFDM) systems

with minimum mean squared error (MMSE) channel estimation. It was also shown that the optimal PDPR that maximizes this lower bound or minimizes the average symbol error rate can significantly increase the capacity compared to a system using a suboptimal PDPR setting. More recently, specifically for MU-MIMO systems, the trade-off between pilot and data symbols was analyzed in [7].

While the above references focused on a single cell system, a series of other works developed models for multi-cell MU-MIMO systems and proposed multi-cell pilot and/or data power control schemes that aim to maximize some system-wide utility functions [8]–[10]. In particular, the results in [8] and [9] indicate that in multi-cell MU-MIMO systems controlling the transmit power of both the pilot and data symbols can drastically improve the spectral and energy efficiency of the system. Those papers, however, do not develop a decentralized scheme that could be used for multi-cell power control. In contrast, the work by [10] proposes a multi-cell game theoretic approach for pilot contamination avoidance, but does not consider the power control problem and that of setting the PDPR.

In this paper we argue that in multi-cell MU-MIMO systems, the PDPR must be set in such a way that multi-cell interference on the data signals as well as on the pilot signals (that is pilot contamination) must be taken into account. Compared to a single-cell system, in a multi-cell system there are new important interdependencies due to the finite sum-power budget, since setting the pilot power for a given user not only affects its own channel estimation and the power left for own data transmission, but it also affects the pilot contamination and the level of inter-cell interference on the data channels. The authors in [11] analyze the impact of pilot contamination on the performance of time division duplexing (TDD) cellular systems, and they show that the pilot contamination causes saturation of the signal-to-interference-plus-noise ratio (SINR) as the number antennas at the BSs increases. To our knowledge, there is no efficient algorithm proposed that takes into account these trade-offs and can be executed in a decentralized fashion in a multi-cell MU-MIMO system.

To address the problem of PDPR-setting in multi-cell systems, we first derive a closed-form expression of mean squared error (MSE) for uplink (UL) received data symbols, and then we use this expression for determining the unique data power that minimizes the individual MSEs. Building on these results, we develop PDPR-setting games that are applicable in multi-cell MU-MIMO systems. The first game is the non-cooperative game $\mathcal{G}_1$, in which each mobile station (MS) has the objective to minimize its own MSE. We prove the existence of a Nash equilibrium of $\mathcal{G}_1$, provide the condition for uniqueness, and propose an algorithm, termed Local Best PDPR (LBP),

P. Zhao and G. Dán are with the KTH Royal Institute of Technology, 11428 Stockholm, Sweden (e-mail : peiyue@kth.se; gyuri@kth.se).

G. Fodor is with the KTH Royal Institute of Technology, 11428 Stockholm, Sweden and also with Ericsson Research, 16480 Stockholm, Sweden (e-mail: gabor.fodor@ericsson.com).

M. Telek is with the Budapest University of Technology and Economics, H-1117 Budapest, Hungary and also with the MTA-BME Information Systems Research Group, H-1117 Budapest, Hungary (e-mail: telek@hit.bme.hu).

that converges to this unique equilibrium. Although the LBP algorithm is attractive thanks to its fast convergence, the selfish behavior of the MSs may lead to a relatively high interference level, which negatively affects the sum MSE performance of the system. Therefore, we also propose the non-cooperative game $\mathcal{G}_2$, in which the MSs are aware of the data interference that they generate to each other, and use that for setting their PDPR. We show that $\mathcal{G}_2$ is a potential game, and we propose a decentralized algorithm, termed the data interference avoidance (DIA) algorithm, for computing a Nash equilibrium of $\mathcal{G}_2$. Numerical results show that DIA improves the fairness among the MSs and the multi-cell sum MSE performance significantly, while the LBP algorithm allows the MSs with good channel condition to achiever lower MSE values.

The rest of the paper is structured as follows. Section II reviews related work and summarizes the contribution of this paper. We introduce the system model and provide a closed-form MSE expression for UL in multi-cell MU-MIMO systems in Sections III and IV. Section V introduces the problem formulation. Sections VI and VII present the LBP algorithm and the DIA algorithm, respectively. Finally, Section VIII discusses numerical results, and Section IX concludes the paper.

II. RELATED WORKS

Due to the importance of PDPR in the performance of MU-MIMO systems, there is a significant interest in investigating the impact of PDPR-setting, and in proposing schemes for optimal or near-optimal PDPR setting.

A. PDPR in MU-MIMO Systems

Problems related to PDPR setting in MU-MIMO systems are addressed in [7], [8], [12]–[17]. The authors in [7] consider a MU-MIMO scenario with time-division duplex operation, and a coherence interval of T symbols spent for channel training, channel estimation, and precoder computation for downlink (DL) transmission. The optimum number of pilot symbols is determined for maximizing the lower bound of the sum-throughput. However, receiver design and the PDPR-setting are out of the scope of that paper. The problem of joint power loading of data and pilot symbols for the purpose of maximizing sum spectral efficiency is addressed in [12], but the impact of PDPR setting at the MU-MIMO receiver is not considered. In contrast, the problem of optimal training period and update interval for maximizing the UL sum-rate is addressed in [15], whereas the receiver structure at the BS is not considered. The authors in [13] consider single-user wireless fading channels, and optimize the pilot overhead. That paper also identifies that the pilot overhead, as well as the spectral efficiency penalty, depends on the square root of the normalized Doppler frequency. More recently, uplink power control and the PDPR-setting problem in MU-MIMO systems are addressed in [14], [8], and [18], assuming practical (zero-forcing (ZF) and MMSE based) multiantenna receiver structures. However, the papers mentioned above focus on centralized approaches, and may not scale well in multi-cell multi-user systems in practice. Scalable decentralized schemes with low complexity are appealing for PDPR setting in multi-cell MU-MIMO systems, and are proposed in [19]–[22]. However, these papers either assume perfect channel state information or they incorporate

CSI errors, but do not address the problem of joint optimization of setting the pilot and data power.

B. Game Theoretic Approaches for Resource Management and Power Control Problems

In addition to the papers mentioned above, a number of game theoretic approaches are applied to power control and resource allocation problems in multi-user systems. The paper [23] uses a Gaussian interference relay game to model the multi-user power control problem for the Gaussian frequency-flat relay channel in the uplink. However, the aspect of PDPR setting under a sum power budget is not considered. Authors in [24] consider the DL transmission of a closed-loop wireless network, while [25] considers the problem of DL power control of small cell base stations under a total power constraint.

Game theoretic approaches are also applied to transmitter-receiver pairs by [26], [27]. The authors in [26] use a non-cooperative game to address the problem of power control, and prove the existence of equilibria by quasi-variational inequality theory. The problem of resource allocation between transmitter-receiver pairs is modeled as player-specific graphical resource allocation games in [27], where equilibria exist and can be computed by polynomial complexity algorithms.

C. Contributions

Based on the above literature survey, we believe that our paper is among the first to propose dynamic and decentralized algorithms for setting the PDPR in multi-cell MU-MIMO systems based on a game-theoretic approach. Our main contributions include the two decentralized PDPR-setting algorithms, which incorporate several important and practically useful results. Specifically, the contributions of this paper are as follows:

- We derive a closed-form expression of the MSE in multi-cell MU-MIMO systems in Proposition 1. We use this expression to derive the unique minimizer of the individual MSEs in Lemma 1.
- We model the PDPR-setting problem for the multi-cell MU-MIMO system as a non-cooperative game $\mathcal{G}_1$, in which the MSs minimize their own MSE in a non-cooperative (selfish) manner, and we propose the LBP algorithm to compute a Nash equilibrium. We prove that the LBP algorithm converges in a finite number of iterations given a convergence threshold in Proposition 2, and we provide a sufficient condition for the uniqueness of the equilibrium in Lemma 5.
- As an alternative to the game $\mathcal{G}_1$, we propose the game $\mathcal{G}_2$, which makes each MS aware of the impact of its own power setting on the other MSs. We prove that $\mathcal{G}_2$ is a potential game in Lemma 7, we propose the DIA algorithm to compute a Nash equilibrium of the game, and we prove the convergence of the proposed algorithm in Proposition 3.

III. SYSTEM MODEL

We consider a multi-cell MU-MIMO system with L cells and K MSs per cell. We assume that the number of antennas at each BS is N_r, and $N_r \gg K$ in practice. Generally, we consider that there are F subcarriers in the coherence bandwidth, and

τ_p and $\tau_d = F - \tau_p$ subcarriers are allocated to the pilot and data symbols, respectively. Specifically, for the kth MS in cell l, considering a total power budget P_{tot}, and transmit power $P_{l,k}^{(p)}$ and $P_{l,k}$ for each pilot and data symbol, respectively, we enforce the constraint

$$\tau_p P_{l,k}^{(p)} + \tau_d P_{l,k} = P_{tot}, \qquad (1)$$

where $1 \le \tau_p, \tau_d < F$. The $N_r \times \tau_p$ matrix of the received pilot signal of the (tagged) κ^{th} MS in cell λ at the serving BS λ can be written as

$$\mathbf{Y}_{\lambda,\kappa}^{(p)} = \underbrace{\sqrt{P_{\lambda,\kappa}^{(p)}} \alpha_{\lambda,\lambda,\kappa} \mathbf{h}_{\lambda,\lambda,\kappa} \mathbf{s}_{\kappa}^T}_{\text{MS } (\lambda,\kappa)\text{'s pilot signal at BS-}\lambda} + \underbrace{\sum_{l \ne \lambda}^{L} \sqrt{P_{l,\kappa}^{(p)}} \alpha_{\lambda,l,\kappa} \mathbf{h}_{\lambda,l,\kappa} \mathbf{s}_{\kappa}^T + \mathbf{N}_{\lambda,\kappa}^p}_{\text{Pilot contamination plus noise to MS } (\lambda,\kappa)}, \qquad (2)$$

where $\mathbf{s}_{\kappa} \in \mathbb{C}^{N_r \times 1}$ is the pilot sequence of the tagged MS (λ,κ), and the product $\alpha_{\lambda,l,\kappa} \mathbf{h}_{\lambda,l,\kappa} \in \mathbb{C}^{N_r \times 1}$ characterizes the large $(\alpha_{\lambda,l,\kappa})$ and small $(\mathbf{h}_{\lambda,l,\kappa})$ scale fading of the wireless channel between MS (l,κ) and BS λ. Notice that in every neighbor cell $l \ne \lambda$, there is exactly one MS (namely MS (l,κ)) that uses the same pilot sequence as MS (λ,κ) and thereby contaminates the pilot signal.

With the least squares channel estimation, the $N_r \times N_r$ covariance matrix of the estimated channel $\hat{\mathbf{h}}_{\lambda,\lambda,\kappa}$ of the tagged user is [28]

$$\mathbf{R}_{\lambda,\lambda,\kappa}(\mathbf{P}) = \mathbf{C}_{\lambda,\lambda,\kappa} + \frac{\sigma_{\text{pc},\lambda,\kappa}^2 (\mathbf{P}_{-(\lambda,\kappa)})}{\alpha_{\lambda,\lambda,\kappa}^2 (P_{tot} - \tau_d P_{\lambda,\kappa})}, \qquad (3)$$

where $\mathbf{P} \triangleq [P_{1,1}, \dots, P_{L,K}] \in \mathbb{R}^{1 \times LK}$ is the vector of data powers of all MSs, $\mathbf{P}_{-(\lambda,\kappa)}$ is the vector of data powers of all MSs except of MS (λ,κ). In the following, depending on the context, we interchangeably use the notation $\mathbf{P}$ and $(P_{\lambda,\kappa}, \mathbf{P}_{-(\lambda,\kappa)})$. In the case of perfectly uncorrelated antennas, $\mathbf{C}_{\lambda,l,\kappa} = c_{\lambda,l,\kappa} \mathbf{I}_{N_r}$ can be assumed, while $\sigma_{\text{pc},\lambda,\kappa}^2 (\mathbf{P}_{-(\lambda,\kappa)})$, the aggregate pilot contamination plus noise (σ_p^2) power affecting the pilot signal of MS (λ,κ) at BS λ, can be written as

$$\sigma_{\text{pc},\lambda,\kappa}^2 (\mathbf{P}_{-(\lambda,\kappa)}) = \underbrace{\left(\sum_{l \ne \lambda}^{L} \frac{(P_{tot} - \tau_d P_{l,\kappa})}{\tau_p} \alpha_{\lambda,l,\kappa}^2 c_{\lambda,l,\kappa} + \sigma_p^2 \right)}_{\triangleq \sigma_{\text{pc},\lambda,\kappa}^2} \mathbf{I}_{N_r}.$$

The conditional distribution of the channel given its estimation $\hat{\mathbf{h}}$ is [28]

$$(\mathbf{h} | \hat{\mathbf{h}}) \sim \mathcal{CN}(\mathbf{D}\hat{\mathbf{h}}, \mathbf{Q}), \qquad (4)$$

where $\mathbf{D} = \mathbf{C}\mathbf{R}^{-1}$ and $\mathbf{Q} = \mathbf{C} - \mathbf{C}\mathbf{R}^{-1}\mathbf{C}$ with $\mathbf{R}$ in (3). In this paper we assume proper antenna spacing and the definition of $\mathbf{D}$ and $\mathbf{Q}$ implies $\mathbf{R}_{\lambda,\lambda,\kappa}(\mathbf{P}) = r_{\lambda,\lambda,\kappa}(\mathbf{P}) \cdot \mathbf{I}$, $\mathbf{D}_{\lambda,\lambda,\kappa}(\mathbf{P}) = d_{\lambda,\lambda,\kappa}(\mathbf{P}) \cdot \mathbf{I}$, $\mathbf{Q}_{\lambda,\lambda,\kappa}(\mathbf{P}) = q_{\lambda,\lambda,\kappa}(\mathbf{P}) \cdot \mathbf{I}$, where the dependence of $r_{\lambda,\lambda,\kappa}$, $d_{\lambda,\lambda,\kappa}$ and $q_{\lambda,\lambda,\kappa}$ on $\mathbf{P}$ has been emphasized.

IV. LINEAR MMSE RECEIVER AND THE MSE

The received data signal from the tagged MS (λ,κ) at the serving BS λ can be written as

$$\mathbf{y}_{\lambda,\kappa} = \underbrace{\alpha_{\lambda,\lambda,\kappa} \mathbf{h}_{\lambda,\lambda,\kappa} \sqrt{P_{\lambda,\kappa}} x_{\lambda,\kappa}}_{\text{MS } (\lambda,\kappa)} + \underbrace{\sum_{k \ne \kappa}^{K} \alpha_{\lambda,\lambda,k} \mathbf{h}_{\lambda,\lambda,k} \sqrt{P_{\lambda,k}} x_{\lambda,k}}_{\text{Other MSs in cell} \lambda}$$

$$+ \underbrace{\sum_{l \ne \lambda}^{L} \sum_{k}^{K} \alpha_{\lambda,l,k} \mathbf{h}_{\lambda,l,k} \sqrt{P_{l,k}} x_{l,k}}_{\text{MSs in other cells except cell } \lambda} + \mathbf{n}_d. \qquad (5)$$

$x_{l,k}$ is the transmitted data symbol by MS (l,k) and the notation $\mathbf{n}_d$ emphasizes the noise on the received data signal.

Due to the power budget constraint, the pilot and data power allocation is constrained such that for the data power levels $P_{l,k} \in \mathcal{P}_d = \left(0, \frac{P_{tot}}{\tau_d}\right)$ holds, where τ_d (as well as τ_p) are identical for all users.

Furthermore, according to [9], [29] and [30] the MMSE receiver $\mathbf{G}_{\lambda,\kappa} \in \mathbb{R}^{1 \times N_r}$ minimizes the MSE of the received data symbols in the presence of CSI errors and takes into account the MU-MIMO interference,

$$\mathbf{G}_{\lambda,\kappa} = g_{\lambda,\kappa} \cdot \hat{\mathbf{h}}_{\lambda,\lambda,\kappa}^H, \qquad (6)$$

where,

$$g_{\lambda,\kappa}(\mathbf{P}) \triangleq$$
$$\alpha_{\lambda,\lambda,\kappa} \sqrt{P_{\lambda,\kappa}} d_{\lambda,\lambda,\kappa} \cdot \left(\alpha_{\lambda,\lambda,\kappa}^2 P_{\lambda,\kappa} \left(d_{\lambda,\lambda,\kappa}^2 ||\hat{\mathbf{h}}_{\lambda,\lambda,\kappa}||^2 + q_{\lambda,\lambda,\kappa} \right) + \right.$$
$$\left. + \underbrace{\sum_{k \ne \kappa}^{K} \alpha_{\lambda,\lambda,k}^2 P_{\lambda,k} c_{\lambda,\lambda,k} + \sum_{l \ne \lambda}^{L} \sum_{k}^{K} \alpha_{\lambda,l,k}^2 P_{l,k} c_{\lambda,l,k} + \sigma_d^2}_{\triangleq \sigma_{\lambda,\kappa}^2 (\mathbf{P}_{-\kappa})} \right)^{-1}. \qquad (7)$$

Accordingly, $\sigma_{\lambda,\kappa}^2 = \sigma_{\lambda,\kappa}^2 (\mathbf{P}_{-(\lambda,\kappa)})$ captures the multi-cell MU-MIMO interference to MS (λ,κ) plus noise. The short notation, $\sigma_{\lambda,\kappa}^2$, is used occasionally for notational convenience.

Based on the data signal model (5) and the receiver $\mathbf{G}_{\lambda,\kappa}$ (7), we consider the MSE of the estimated data symbols of the tagged MS (λ,κ),

$$\text{MSE}_{\lambda,\kappa}(\mathbf{P}) = \mathbb{E}\{|\mathbf{G}_{\lambda,\kappa} \mathbf{y}_{\lambda,\kappa} - x_{\lambda,\kappa}|^2\}. \qquad (8)$$

Furthermore, in this case, we can obtain the unconditional MSE as a function of the data power $\mathbf{P}$ of all the MSs as follows:

Proposition 1. *In a multi-cell MU-MIMO system with pilot contamination, the unconditional MSE of the received data symbols of MS (λ,κ) when BS λ uses MMSE receiver $\mathbf{G}_{\lambda,\kappa}$ is*

$$\text{MSE}_{\lambda,\kappa}(\mathbf{P}) = \mu_{\lambda,\kappa} e^{\mu_{\lambda,\kappa}} E_{in}(N_r, \mu_{\lambda,\kappa}), \qquad (9)$$

where $\mu_{\lambda,\kappa}$, is a function of $\mathbf{P}$, and is defined by
$$\mu_{\lambda,\kappa} = \mu_{\lambda,\kappa}(\mathbf{P}) \triangleq \frac{q_{\lambda,\lambda,\kappa}(P_{\lambda,\kappa}) \alpha_{\lambda,\lambda,\kappa}^2 P_{\lambda,\kappa} + \sigma_{\lambda,\kappa}^2 (\mathbf{P}_{-(\lambda,\kappa)})}{d_{\lambda,\lambda,\kappa}^2 (P_{\lambda,\kappa}) \alpha_{\lambda,\lambda,\kappa}^2 P_{\lambda,\kappa} r_{\lambda,\lambda,\kappa}(P_{\lambda,\kappa})}, \qquad (10)$$

and $E_{in}(n, z) \triangleq \int_1^{\infty} \frac{e^{-zt}}{t^n} dt$ is the standard exponential integral function.

The proof is provided in Appendix A.

V. PROBLEM FORMULATION

Now we are ready to formulate the MU-MIMO PDPR setting (MPS) problem in multi-cell systems. Due to the sum power

3

constraint (1), setting PDPR of a MS is equivalent to setting its data power $P_{\lambda,\kappa}$. Therefore we formulate the MPS problem as to compute a data power allocation $\mathbf{P}$ to minimize the sum MSE of MSs,

$$
\begin{aligned}
\underset{\mathbf{P}}{\text{minimize}} \quad & \sum_{l=1}^{L}\sum_{k=1}^{K}\text{MSE}_{l,k}(\mathbf{P}) \\
\text{subject to} \quad & \tau_d P_{l,k} > 0, \ \forall l, k \\
& \tau_d P_{l,k} < P_{tot}, \ \forall l, k
\end{aligned}
\tag{P1}
$$

Problem (P1) is difficult to solve in general. Though later we show that $\text{MSE}_{l,k}(\mathbf{P})$ of MS (l, k) is quasi-convex with respect to its own data power, the objective function of (P1) is not necessarily quasi-convex with respect to $\mathbf{P}$, which is required to solve (P1) as a quasi-convex optimization problem. Even if (P1) can be solved as a quasi-convex optimization problem, general techniques, for example, cutting plane methods and bisection search may not scale well for a large sized system [31, Chapter 4]. More importantly, due to practical real-world constraints we are interested in decentralized PDPR setting algorithms that operate in multi-cell MU-MIMO systems. For these reasons, in this work we propose game theoretic approaches to developing decentralized algorithms, which, as the numerical results show, approximate the optimal solution very well.

VI. LOCAL BEST PDPR ALGORITHM

Game theory considers the decision making of a set of individuals, referred to as players, that interact with each other to optimize their own objectives (e.g., utilities or payoffs), for which each player can choose from a set of available decisions, referred to as an action set. It is appealing to use game theory to model decentralized PDPR setting, where the MSs have conflict of interest in terms of data interference and pilot contamination. We are interested in computing a Nash Equilibrium as a solution, in which no player can further improve its objective by changing its action.

In this section we develop a game theoretic algorithm for decentralized PDPR setting in multi-cell MU-MIMO systems. To start with, we first explore the existence and two important properties of the unique minimizer of the individual MSE, which allows us to develop an iterative decentralized algorithm to compute the PDPR of each MS. In the proposed algorithm, termed LBP, each MS updates its data power iteratively to minimize its own MSE until the improvement of MSE falls below a threshold. Further results show that LBP converges, and the convergence is unique if a well-defined condition is satisfied.

A. The Unique Minimizer of Individual MSE

As a first step, we introduce the minimizer of the MSE of each MS (λ, κ).

Lemma 1. *In a multi-cell MU-MIMO system with pilot contamination, given the data power allocation $\mathbf{P}_{-(\lambda,\kappa)}$ of the other MSs, the data power $P_{\lambda,\kappa}^{\star}(\mathbf{P}_{-(\lambda,\kappa)})$ that minimizes the MSE of MS (λ, κ) is*

$$
P_{\lambda,\kappa}^{\star}(\mathbf{P}_{-(\lambda,\kappa)}) = \frac{P_{tot}}{\tau_d + M(\mathbf{P}_{-(\lambda,\kappa)})},
\tag{11}
$$

Algorithm 1: Local Best PDPR Algorithm

Input: MSE improvement threshold ϵ
1 Initial data power $P_{\lambda,\kappa}^{(0)} = P_{\lambda,\kappa}^{\star}(\mathbf{0})$
2 $i = 0$
3 **while** $P_{\lambda,\kappa}^{(i)} \neq P_{\lambda,\kappa}^{(i-1)}$, $\forall \kappa \in \mathcal{K}$ **do**
4   BS sends $\sigma_{\text{pc},\lambda,\kappa}^{2}(\mathbf{P}_{-(\lambda,\kappa)})$ and $\sigma_{\lambda,\kappa}^{2}(\mathbf{P}_{-(\lambda,\kappa)})$ to MS (λ, κ)
5   **for** $\kappa \in \mathcal{K}$ *and* $\lambda \in \mathcal{L}$ **do**
6   **if** $\text{MSE}_{\lambda,\kappa}\left(P_{\lambda,\kappa}^{(i-1)}, \mathbf{P}_{-(\lambda,\kappa)}^{(i-1)}\right) - \text{MSE}_{\lambda,\kappa}\left(P_{\lambda,\kappa}^{\star}(\mathbf{P}_{-(\lambda,\kappa)}^{(i-1)}), \mathbf{P}_{-(\lambda,\kappa)}^{(i-1)}\right) > \epsilon$ **then**
7          $P_{\lambda,\kappa}^{(i)} = P_{\lambda,\kappa}^{\star}(\mathbf{P}_{-(\lambda,\kappa)}^{(i-1)})$
8   **else** $P_{\lambda,\kappa}^{(i)} = P_{\lambda,\kappa}^{(i-1)}$
9    $i = i + 1$

Output: Data power allocation $\mathbf{P}$.

---

where $M(\mathbf{P}_{-(\lambda,\kappa)}) = \sqrt{\tau_d \dfrac{\frac{c_{\lambda,\kappa}P_{tot}\alpha_{\lambda,\kappa}^{2}}{\sigma_{\lambda,\kappa}^{2}(\mathbf{P}_{-(\lambda,\kappa)})} + \tau_d}{\frac{c_{\lambda,\kappa}P_{tot}\alpha_{\lambda,\kappa}^{2}}{\sigma_{\text{pc},\lambda,\kappa}^{2}(\mathbf{P}_{-(\lambda,\kappa)})} + 1}}$.

The proof is provided in Appendix B. For convenience, we refer to (11) as the best response function. Further investigation shows two important properties of the best response function, which are useful for the development of LBP.

Lemma 2. *The best response function $P_{\lambda,\kappa}^{\star}(\mathbf{P}_{-(\lambda,\kappa)})$ of the data power for MS (λ, κ) is a strictly increasing function of the data power $\forall P_{l,j} \neq \forall P_{\lambda,\kappa}$.*

The proof of Lemma 2 is in Appendix C. Furthermore, $P_{\lambda,\kappa}^{\star}(\mathbf{P}_{-(\lambda,\kappa)})$ is bounded, as stated in the next lemma.

Lemma 3. *The best response function $P_{\lambda,\kappa}^{\star}(\mathbf{P}_{-(\lambda,\kappa)})$ of the data power for MS (λ, κ) is bounded by*

$$
0 < \underline{P_{\lambda,\kappa}} \leq P_{\lambda,\kappa}^{\star}(\mathbf{P}_{-(\lambda,\kappa)}) < \overline{P_{\lambda,\kappa}} < \frac{P_{tot}}{\tau_d},
\tag{12}
$$

where $\underline{P_{\lambda,\kappa}} = \lim_{\Delta \to 0} P_{\kappa}^{\star}(\Delta \mathbf{e})$ *and* $\overline{P_{\lambda,\kappa}} = \lim_{\Delta \to \frac{P_{tot}}{\tau_d}} P_{\kappa}^{\star}(\Delta \mathbf{e})$.

The proof is provided in Appendix D. Furthermore, we prove the following results.

Lemma 4. $\left|\frac{\partial \text{MSE}_{\lambda,\kappa}(\mathbf{P})}{\partial P_{\lambda,\kappa}}\right|$ *is a bounded function on* $[\underline{P_{\lambda,\kappa}}, \overline{P_{\lambda,\kappa}}]$, *and* $max\{|\frac{\partial \text{MSE}_{\lambda,\kappa}(\mathbf{P})}{\partial P_{\lambda,\kappa}}|\}$ *exists on* $[\underline{P_{\lambda,\kappa}}, \overline{P_{\lambda,\kappa}}]$.

The proof is provided in Appendix E . The lemmas above show that when the data power setting of the other MSs is fixed, a MS can minimize its own MSE by setting its own data power independently, which provides the basis to model the PDPR problem as a non-cooperative game.

B. Local Best PDPR Algorithm

We model the problem of setting the data power as a non-cooperative game $\mathcal{G}_1$, where the players are the MSs, and the action of each player is to set its data power $P_{\lambda,\kappa}$. In $\mathcal{G}_1$ the payoff function of each MS (λ, κ) is $\text{MSE}_{\lambda,\kappa}(\mathbf{P})$. We are

Table I: Numerical Example for Contractivity Based on (16)

Parameter or Expression	Value
L	2
K	2
$c_{1,l,j}, \quad \forall j, \, l$	1
τ_d	6
P_{tot}	24 dBm $\approx$ 250 mW
$P_{l,j}, \quad \forall j, l$	120 mW
P_{tot}/τ_d	25 mW
$\sigma_{1,1}^2\big(\mathbf{P}_{-(1,1)}\big)$	$1.6360 \cdot 10^{-12}$
$\sigma_{pc,1,1}^2\big(\mathbf{P}_{-(1,1)}\big)$	$7.3110 \cdot 10^{-13}$
$\dfrac{\partial P_{\lambda,\kappa}^\star\big(\mathbf{P}_{-(\lambda,\kappa)}\big)}{\partial P_{l,j}}$	$\dfrac{\partial P_{\lambda,\kappa}^\star(\mathbf{P}_{-(\lambda,\kappa)})}{\partial P_{1,2}} = 1.4302 \cdot 10^{-10}$ $\dfrac{\partial P_{\lambda,\kappa}^\star(\mathbf{P}_{-(\lambda,\kappa)})}{\partial P_{2,1}} = 1.9141 \cdot 10^{-12}$ $\dfrac{\partial P_{\lambda,\kappa}^\star(\mathbf{P}_{-(\lambda,\kappa)})}{\partial P_{2,2}} = 2.7992 \cdot 10^{-13}$
$\sum_l^L \sum_j^K \dfrac{\partial P_{\lambda,\kappa}^\star\big(\mathbf{P}_{-(\lambda,\kappa)}\big)}{\partial P_{l,j}}$	$2.8433 \cdot 10^{-10}$

interested in a data power setting in which no MS has an incentive to change its data power, i.e., a Nash equilibrium of the game, defined as follows.

Definition 1. *An ϵ-Nash equilibrium of the strategic game $\mathcal{G}_1$ is a data power allocation profile $\mathbf{P}$ such that for all MS (λ, κ),*

$$\mathrm{MSE}_{\lambda,\kappa}(P_{\lambda,\kappa}, \mathbf{P}_{-(\lambda,\kappa)}) \leq \mathrm{MSE}_{\lambda,\kappa}(P'_{\lambda,\kappa}, \mathbf{P}_{-(\lambda,\kappa)}) + \epsilon, \ \forall P'_{\lambda,\kappa} \in \mathcal{P}_d. \tag{13}$$

A pure strategy Nash equilibrium is an ϵ-Nash equilibrium for $\epsilon = 0$.

Based on the results in Lemmas 2 and 3, we propose the LBP algorithm to compute a data power allocation for $\mathcal{G}_1$, as described in Algorithm 1. Line 1 initializes the algorithm by setting the data power of each MS (λ, κ) as their best response data power with respect to the noise power to BS λ. Then, in iteration i, the BSs measure and send $\sigma_{pc,\lambda,\kappa}^2\big(\mathbf{P}_{-(\lambda,\kappa)}\big)$ and $\sigma_{\lambda,\kappa}^2\big(\mathbf{P}_{-(\lambda,\kappa)}\big)$ to each MS, which allows them to compute their best response data power $P_{\lambda,\kappa}^\star\big(\mathbf{P}_{-(\lambda,\kappa)}^{(i-1)}\big)$ according to (4). If the MSE improvement $\mathrm{MSE}_{\lambda,\kappa}\Big(P_{\lambda,\kappa}^{(i-1)}, \mathbf{P}_{-(\lambda,\kappa)}^{(i-1)}\Big) - \mathrm{MSE}_{\lambda,\kappa}\Big(P_{\lambda,\kappa}^\star(\mathbf{P}_{-(\lambda,\kappa)}^{(i-1)}), \mathbf{P}_{-(\lambda,\kappa)}^{(i-1)}\Big)$ by $P_{\lambda,\kappa}^\star\big(\mathbf{P}_{-(\lambda,\kappa)}^{(i-1)}\big)$ is higher than a threshold ϵ, then MS (λ, κ) updates its data power $P_{\lambda,\kappa}^{(i)}$ to $P_{\lambda,\kappa}^\star\big(\mathbf{P}_{-(\lambda,\kappa)}^{(i-1)}\big)$, otherwise it keeps its current data power. When all MSs stop updating their data power, respectively, LBP terminates. Since the MSs update their data powers simultaneously, LBP allows fast operation at the cost of synchronizing all the MSs, and thus the computation time of LBP in each iteration remains the same as the number of cells and MSs increase. To implement LBP, a practical signaling scheme can be that each BS executes line 4 of Algorithm 1 periodically, and then each MS executes lines 6-8 simultaneously during each interval.

C. Convergence of LBP and Equilibrium Uniqueness

The proposed LBP algorithm is a decentralized algorithm with simple operations, and would be appealing if it converged to a Nash equilibrium of $\mathcal{G}_1$. In what follows, we first prove the convergence of LBP to an equilibrium, and then we derive a condition for the unique convergence of LBP.

Proposition 2. *For any $\epsilon > 0$ LBP converges to an ϵ-Nash equilibrium in a finite number of iterations. Furthermore, for $\epsilon = 0$ it converges to a pure Nash equilibrium.*

Proof. According to Algorithm 1, $P_{\lambda,\kappa}^{(0)} > 0$, thus $P_{\lambda,\kappa}^{(1)} \geq P_{\lambda,\kappa}^{(0)}$. Consider now iteration i, and assume that $\mathbf{P}_{-(\lambda,\kappa)}^{(i)} \geq \mathbf{P}_{-(\lambda,\kappa)}^{(i-1)}$ holds for $i = 1$. Then, by Lemma 2 we have $P_{\lambda,\kappa}^{(i+1)} \geq P_{\lambda,\kappa}^{(i)}$, and $\mathbf{P}_{-(\lambda,\kappa)}^{(i+1)} \geq \mathbf{P}_{-(\lambda,\kappa)}^{(i)}$ for all MSs. Thus, the sequence $\{P_{\lambda,\kappa}^{(i)}\}$ is a monotone increasing sequence. Besides, as Lemma 3 shows $\{P_{\lambda,\kappa}^{(i)}\}$ is bounded. By the monotone convergence theorem, $\{P_{\lambda,\kappa}^{(i)}\}$ is convergent, which proves that the LBP converges. By Lemma 4 $\max\{|\frac{\partial \mathrm{MSE}_{\lambda,\kappa}(\mathbf{P})}{\partial P_{\lambda,\kappa}}|\}$ exists, and according to the mean value theorem [32, Chapter 6.3], if MS (λ, κ) updates its data power at iteration i, it increases its data power by at least $\epsilon \cdot (\max\{|\frac{\partial \mathrm{MSE}_{\lambda,\kappa}(\mathbf{P})}{\partial P_{\lambda,\kappa}}|\})^{-1}$. Since $\{P_{\lambda,\kappa}^{(i)}\}$ is bounded, LBP converges in a finite number of iterations. Furthermore, when LBP terminates, the criteria in line 6 of Algorithm 1 satisfies (13) of Definition 1, and therefore the resulting PDPR forms an ϵ-Nash equilibrium. Following the same argument it is easy to see that LBP converges to a pure Nash equilibrium when $\epsilon = 0$. $\qquad\square$

In what follows, we continue with proving the uniqueness of the convergence of LBP. To start with, we define $\mathbf{f} : \mathbb{R}^{1 \times KL} \mapsto \mathbb{R}^{1 \times KL}$ as a mapping from $\mathbf{P}$ to $\mathbf{P}^\star$ and prove that $\mathbf{f}$ is a contraction mapping in $\mathcal{P}_d^{1 \times KL}$ if an easy to check condition holds. Consequently, it has a unique fixed point and LBP converges to this unique fixed point.

$$\mathbf{f}(\mathbf{P}) \triangleq \big[P_{1,1}^\star(P_{1,1}, \mathbf{P}_{-(1,1)}), \ldots, P_{K,L}^\star(P_{K,L}, \mathbf{P}_{-(K,L)}) \big], \tag{14}$$

where $P_{\lambda,\kappa}^\star\big(P_{\lambda,\kappa}, \mathbf{P}_{-(\lambda,\kappa)}\big)$ is independent of $P_{\lambda,\kappa}$. Furthermore, define the $KL \times KL$ matrix $\mathbf{F}(\mathbf{P})$ so that its $(i,j)^{th}$ element is

$$\mathbf{F}(\mathbf{P})_{ij} \triangleq \frac{\partial}{\partial p_i(\mathbf{P})} f_j(\mathbf{P}), \tag{15}$$

where $f_j(\mathbf{P})$ and $p_j(\mathbf{P})$ denotes the jth element of row vector $\mathbf{f}(\mathbf{P})$ and $\mathbf{P}$, respectively. Note that $\mathbf{F}(\mathbf{P})_{ii} = 0$.

Lemma 5. *The best response power allocation as defined by (14) is a contraction mapping if the following condition holds for $\forall \kappa$ and $\forall \, \mathbf{P} \in \mathcal{P}_d^{1 \times KL}$,*

$$\sum_{l=1}^L \sum_{k=1}^K \frac{\partial P_{\lambda,\kappa}^\star\big(\mathbf{P}_{-(\lambda,\kappa)}\big)}{\partial P_{l,k}} \leq \eta < 1, \quad \forall \lambda, \, \kappa, \tag{16}$$

where $\eta < 1$ is a number arbitrarily close to 1.

The proof is provided in Appendix F. Note that the condition stated in Lemma 5 is mild in the sense that it is always fulfilled in practice. As an example, Table I shows the parameters for a

2-cell system with 2 MSs in each cell; the evaluated left hand side of condition (16) is $2.8433 \cdot 10^{-10} \ll 1$.

VII. Data Interference Avoidance Algorithm

According to Lemma 2, the behavior of a MS in LBP is selfish in the sense that a MS increases its data power whenever the data power of any other MS increases, and the increased data interference may further harm the MSE of the other MSs. Therefore, it is appealing to develop an approach where each MS also considers the impact of its power setting on the other MSs. We address this in the following by proposing an alternative cost function for the MSs.

A. Non-selfish Data Power Setting Game

To consider an alternative cost function, we define the non-cooperative game $\mathcal{G}_2$, in which the players are the MSs, and the action of each player is to set its data power $P_{\lambda,\kappa}$, like in game $\mathcal{G}_1$. Nonetheless, in game $\mathcal{G}_2$ the cost function $u_{\lambda,\kappa}(\mathbf{P})$ of each MS (λ, κ) is defined as

$$u_{\lambda,\kappa}(\mathbf{P}) = \gamma_{\lambda,\kappa}(\mathbf{P}) + \theta_{\lambda,\kappa}(\mathbf{P}), \tag{17}$$

where $\gamma_{\lambda,\kappa}(\mathbf{P})$ is the reciprocal of the signal-to-interference ratio (SIR) of the tagged MS (λ, κ),

$$\gamma_{\lambda,\kappa}(\mathbf{P}) = \left(\frac{\alpha_{\lambda,\lambda,\kappa}^2 P_{\lambda,\kappa}}{\sum_{k \neq \kappa}^K \alpha_{\lambda,\lambda,k}^2 P_{\lambda,k} + \sum_{l \neq \lambda}^L \sum_k^K \alpha_{\lambda,l,k}^2 P_{l,k}} \right)^{-1}, \tag{18}$$

and $\theta_{\lambda,\kappa}(\mathbf{P})$ is the SIR of other MSs that are affected by MS (λ, κ),

$$\theta_{\lambda,\kappa}(\mathbf{P}) = P_{\lambda,\kappa} \left(\sum_{k \neq \kappa}^K \frac{\alpha_{\lambda,\lambda,\kappa}^2}{\alpha_{\lambda,\lambda,k}^2 P_{\lambda,k}} + \sum_{l \neq \lambda}^L \sum_k^K \frac{\alpha_{l,\lambda,\kappa}^2}{\alpha_{\lambda,l,k}^2 P_{l,k}} \right). \tag{19}$$

In game $\mathcal{G}_2$ each MS sets its data power to minimize its cost function $u_{\lambda,\kappa}(\mathbf{P})$. The cost function (17) makes each MS set its data power in a non-selfish way such that when MS (λ, κ) increases its data power to improve its own SIR, MS (λ, κ) receives a punishment for interfering with the data signal of other MSs.

The following important result shows that the cost function $u_{\lambda,\kappa}(\mathbf{P})$ is convex, and there exists a unique minimizer of $u_{\lambda,\kappa}(\mathbf{P})$, referred to as the best response function of an MS in $\mathcal{G}_2$.

Lemma 6. $u_{\lambda,\kappa}(\mathbf{P})$ is a convex function over $P_{\lambda,\kappa}$, and there exists a unique $P_{\lambda,\kappa}^\Delta \in \mathcal{P}_d$ that minimizes $u_{\lambda,\kappa}(\mathbf{P})$, for a given $\mathbf{P}_{-(\lambda,\kappa)}$.

$$P_{\lambda,\kappa}^\Delta(\mathbf{P}_{-(\lambda,\kappa)}) = \min\left(a^\Delta, \frac{P_{tot}}{\tau_d}\right), \tag{20}$$

where

$$a^\Delta = \sqrt{\frac{\sum_{k \neq \kappa}^K \alpha_{\lambda,\lambda,k}^2 P_{\lambda,k} + \sum_{l \neq \lambda}^L \sum_k^K \alpha_{\lambda,l,k}^2 P_{l,k}}{\sum_{k \neq \kappa}^K \frac{\alpha_{\lambda,\lambda,\kappa}^4}{\alpha_{\lambda,\lambda,k}^2 P_{\lambda,k}} + \sum_{l \neq \lambda}^L \sum_k^K \frac{\alpha_{l,\lambda,\kappa}^2 \alpha_{\lambda,\lambda,\kappa}^2}{\alpha_{\lambda,l,k}^2 P_{l,k}}}}.$$

Proof. First we prove the convexity of $u_{\lambda,\kappa}(\mathbf{P})$ by noticing that the second derivative of $u_{\lambda,\kappa}(\mathbf{P})$,

$$\frac{\partial^2 u_{\lambda,\kappa}(\mathbf{P})}{\partial P_{\lambda,\kappa}^2} = \frac{2\left(\sum_{k \neq \kappa}^K \alpha_{\lambda,\lambda,k}^2 P_{\lambda,k} + \sum_{l \neq \lambda}^L \sum_k^K \alpha_{\lambda,l,k}^2 P_{l,k}\right)}{\alpha_{\lambda,\lambda,\kappa}^2 P_{\lambda,\kappa}^3} \tag{21}$$

is larger than zero and therefore $u_{\lambda,\kappa}(\mathbf{P})$ is a convex function over $P_{\lambda,\kappa}$. Solving $\frac{\partial u_{\lambda,\kappa}(\mathbf{P})}{\partial P_{\lambda,\kappa}} = 0$ shows that there is only one solution, which is a^Δ, thus $P_{\lambda,\kappa}^\Delta$ is the unique minimizer of $u_{\lambda,\kappa}(\mathbf{P})$ in $\mathcal{P}_d$, for a given $\mathbf{P}_{-(\lambda,\kappa)}$. $\square$

For a fair comparison with the LBP algorithm we introduce

$$P_{\lambda,\kappa}^+\left(\mathbf{P}_{-(\lambda,\kappa)}\right) \triangleq \min\left(P_{\lambda,\kappa}^\Delta\left(\mathbf{P}_{-(\lambda,\kappa)}\right), \max_{l \in \mathcal{L}, k \in \mathcal{K}} \overline{P_{l,k}}\right). \tag{22}$$

B. Data Interference Avoidance (DIA) Algorithm

We are now ready to introduce the DIA algorithm. The pseudo-code of the algorithm is shown in Algorithm 2. In line 1, every MS sets its data power to half of the full power, which is reasonable since the MSs have no knowledge about the power setting of the other MSs in the initialization stage. Next, in lines 5-9, every MS updates its data power iteratively. Specifically, in line 5, each BS sends the data power setting $\mathbf{P}_{-(\lambda,\kappa)}^{(i-1)}$ of all the other MSs to MS (λ, κ) to compute its best response data power $P_{\lambda,\kappa}^+(\mathbf{P}_{-(\lambda,\kappa)}^{(i-1)})$. If $P_{\lambda,\kappa}^+(\mathbf{P}_{-(\lambda,\kappa)}^{(i-1)})$ improves the cost function of MS (λ, κ) by at least ϵ, MS (λ, κ) updates its data power according to line 7. If $P_{\lambda,\kappa}^+(\mathbf{P}_{-(\lambda,\kappa)}^{(i-1)})$ improves the cost function of MS (λ, κ) by less than ϵ, MS (λ, κ) keeps its current data power setting. DIA terminates when no MS updates its data power. Since MSs in DIA update their data power simultaneously, the complexity of DIA in each iteration does not increase with the number of cells and MSs.

C. Convergence of the DIA Algorithm

Before we continue to investigate the convergence of the DIA algorithm, let us recall the definition of an exact potential function from (Definition 25, [33]).

Definition 2. Game $\mathcal{G}_2$ is an exact potential game, if and only if there exists a function $\Psi : \mathcal{P}^N \to \mathbb{R}$ such that for any data power $P_{l,k}$ and $P_{l,k}' \in \mathcal{P}_d$ the following holds for any $k \in \mathcal{K}$ and for any $l \in \mathcal{L}$,

$$\Psi\left(P_{l,k}, \mathbf{P}_{-(l,k)}\right) - \Psi\left(P_{l,k}', \mathbf{P}_{-(l,k)}\right)$$
$$= u_{l,k}\left(P_{l,k}, \mathbf{P}_{-(l,k)}\right) - u_{l,k}\left(P_{l,k}', \mathbf{P}_{-(l,k)}\right). \tag{23}$$

Function $\Psi(\mathbf{P})$ is an exact potential function for $\mathcal{G}_2$.

In what follows, we prove that the game $\mathcal{G}_2$ is an exact potential game by showing that $\mathcal{G}_2$ has a potential function.

Lemma 7. The game $\mathcal{G}_2$ admits the exact potential function

$$\Psi(\mathbf{P}) = \frac{1}{2} \sum_{l=1}^L \sum_{k=1}^K u_{l,k}(\mathbf{P}), \tag{24}$$

and thus $\mathcal{G}_2$ is an exact potential game.

Algorithm 2: Data Interference Avoidance (DIA) Algorithm

---
1 Initial data power $P_{\lambda,\kappa}^{(0)} = \frac{P_{tot}}{2\tau_d}$
2 $i = 0$
3 **while** $P_{\lambda,\kappa}^{(i)} \neq P_{\lambda,\kappa}^{(i-1)}, \; \forall \kappa \in \mathcal{K} \; and \; \forall \lambda \in \mathcal{L}$ **do**
4   **for** $\lambda \in \{1,\ldots,L\} \; and \; \kappa \in \{1,\ldots,K\}$ **do**
5   BS sends $\mathbf{P}_{-(\lambda,\kappa)}^{(i-1)}$ and $\alpha_{i,l,\kappa}$ to MS (λ,κ)
6   **if** $u_{\lambda,\kappa}\left(P_{\lambda,\kappa}^{(i-1)}, \mathbf{P}_{-(\lambda,\kappa)}^{(i-1)}\right) -$
        $u_{\lambda,\kappa}\left(P_{\lambda,\kappa}^{+}(\mathbf{P}_{-(\lambda,\kappa)}^{(i-1)}), \mathbf{P}_{-(\lambda,\kappa)}^{(i-1)}\right) > \epsilon$ **then**
7 $P_{\lambda,\kappa}^{(i)} = P_{\lambda,\kappa}^{+}(\mathbf{P}_{-(\lambda,\kappa)}^{(i-1)})$
8   **else**
9 $P_{\lambda,\kappa}^{(i)} = P_{\lambda,\kappa}^{(i-1)}$
10 $i = i + 1$

Output: Data power allocation $\mathbf{P}$.

The proof is provided in Appendix G, and the following result is immediate.

Proposition 3. *The DIA algorithm converges to an ϵ-Nash equilibrium of $\mathcal{G}_2$ in a finite number of iterations.*

Proof. According to Lemma 6, $P_{\lambda,\kappa}^{+}(P_{-(\lambda,\kappa)}) \in \mathcal{P}_d$ is the unique minimizer of the cost function $u_{\lambda,\kappa}(P_{\lambda,\kappa}, P_{-(\lambda,\kappa)})$ according to $P_{-(\lambda,\kappa)}$. Therefore, the cost function of MS (λ,κ) is bounded from below. Thus, $\mathcal{G}_2$ is a bounded potential game (Section 4, [34]). Since $\mathcal{G}_2$ is a bounded potential game, $\mathcal{G}_2$ possesses an ϵ Nash equilibrium (Lemma 4.1, [34]), and the best reply and better reply dynamics converge to an ϵ-Nash equilibrium of $\mathcal{G}_2$ (Corollary 2.4, [35]). Observe, that the DIA algorithm lets one MS perform a best response upon every iteration, if the best response provides an improvement of at least ϵ, hence convergence follows. Since $u_{\lambda,\kappa}(P_{\lambda,\kappa}, P_{-(\lambda,\kappa)})$ is bounded from below on $\mathcal{P}_d$, $\Psi(\mathbf{P})$ is bounded from below. Therefore, the DIA algorithm converges in a finite number of iterations, $\forall \epsilon > 0$. $\square$

VIII. NUMERICAL RESULTS

In this section, we consider various MU-MIMO scenarios, and present numerical results. We first verify a few important properties of the MSE with and without pilot contamination, then evaluate the proposed LBP and DIA algorithms in terms of the achieved MSE and the corresponding pilot and data power setting in a three-cell scenario. Finally, we examine the convergence of the DIA and LBP algorithms. The simulation parameters are summarized in Table II.

A. Properties of the MSE

We first consider a single cell system with two MSs and $N_r = 100$. The pathloss between each MS and the BS is 73.8 dB. Figure 1(a) shows the MSE of MS $(1,1)$ as a function of its own data power $\tau_d P_{1,1}$, with $\tau_d P_{1,2} = 10$mW, 120 mW, and 240 mW, respectively. The results show that as the power of MS $(1,2)$ increases, the MSE of MS $(1,1)$ increases, since increasing $\tau_d P_{1,2}$ increases the data interference of MS $(1,1)$. Next, we consider a two-cell system with one MS per cell. The

Table II: System Parameters

Parameter	Value
Number of antennas at the BS	$N_r = 10, 100, 500$
Total number of symbols	$F = 12$
Number of data symbols	$\tau_d = 8$
Number of pilot symbols	$F - \tau_d$
Power budget	$P_{tot} = 24$ dBm
Thermal noise density	-174 dBm/Hz

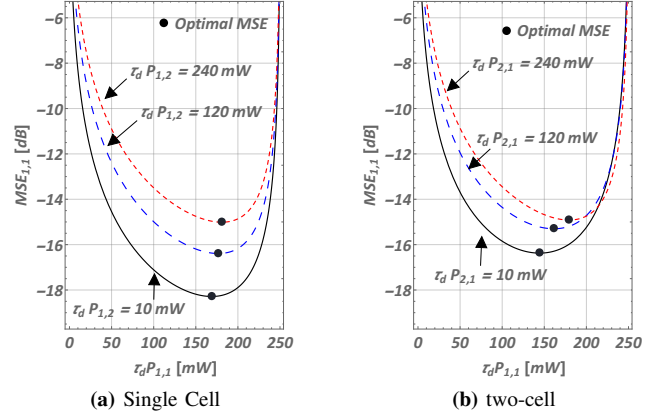**(a)** Single Cell   **(b)** two-cell

Figure 1: MSE of MS $(1,1)$ as a function of $P_{1,1}$, with and without pilot contamination. Due to the pilot contamination, for the same $P_{1,1}$ and data interference, MS $(1,1)$ achieves a worse MSE in the two-cell system than in the single cell system.

pathloss between any MS and any BS is again 73.8 dB. To evaluate the impact of pilot contamination, we assume that the two MSs are using the same pilot sequence. Figure 1(b) shows the MSE of MS $(1,1)$ as a function of its own data power, with $\tau_d P_{2,1} = 10$mW, 120 mW, and 240 mW, respectively. Observe that due to the pilot contamination, with the same data interference, MS $(1,1)$ achieves a higher MSE in the two-cell system than in the single cell system. It is also interesting to see that when $\tau_d P_{1,1} > 220$ mW, increasing $\tau_d P_{2,1}$ from 120 mW to 240 mW reduces $\text{MSE}_{1,1}$, which is in contrast to the single cell system. The reason for this behavior in the two-cell system is that when MS $(1,1)$ allocates more power to the data signal, it allocates less power to the pilot signal and thus becomes more sensitive to pilot contamination. In Figure 1(a) and 1(b), the black dot on each curve shows the optimal MSE that MS $(1,1)$ can achieve and the corresponding data power setting. We observe in both cases that as the data power of the other MS increases, the optimal power setting of MS $(1,1)$ increases, which is consistent with Lemma 2.

B. MSE Performance

To evaluate the performance of the proposed LBP and DIA algorithms, we consider a three-cell system serving 8 users, where the BS is equipped with 10, 100, or 500 antennas. Figure 2 shows the CDF of the sum MSE of the MSs for the three-cell system. The results show that the DIA algorithm outperforms the LBP algorithm in terms of the sum MSE by about 1 dB when $N_r = 10$. Furthermore, increasing the number of antennas increases the performance gain of DIA. When $N_r = 500$, for example, the DIA brings about 5 dB gains to
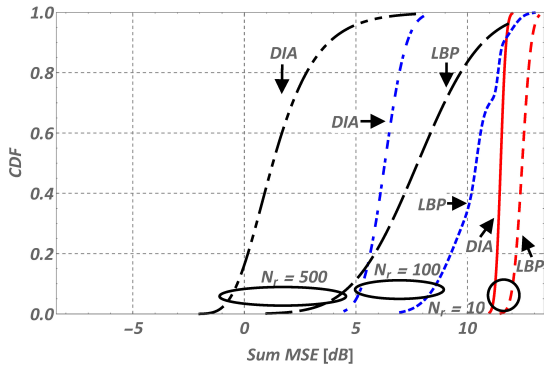
Figure 2: The CDF of sum MSE for a three-cell system, with $N_r = 10, 100$, and 500. DIA outperforms LBP at the cost of requiring more CSI.
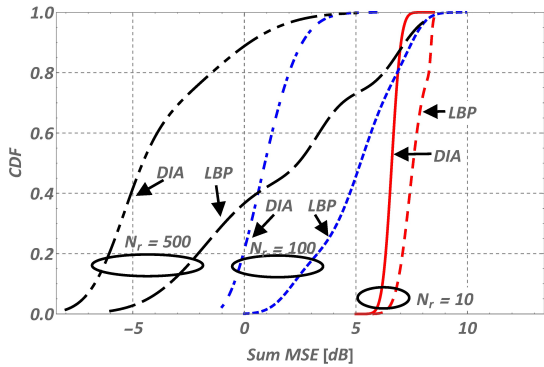

Figure 3: The CDF of individual MSE for a three-cell system, with $N_r = 10, 100$, and 500. In DIA about 80 percent of the MSs achieves a lower MSE than in LBP, and DIA also achieves a better fairness than LBP.

Figure 4: The CDF of sum MSE for a single cell system, with $N_r = 10, 100$, and 500. The performance gap between DIA and LBP in single cell system is smaller than that in three-cell system.

Figure 5: The CDF of sum MSE for a three-cell system with MSs placed at the cell edge, $K = 2$ and 8, and $N_r = 100$. DIA performs close to the optimal solution, and both DIA and LBP outperform the fixed power allocation scheme.

the system. This can be explained by the different behaviors of the MSs in the two algorithms.

Using LBP, each MS minimizes its own MSE at the cost of generating interference to the data signal of the other MSs. Therefore, as LBP progresses, the received data interference of every MS increases. Although LBP allows each MS to choose the data power that minimizes its own MSE, the system suffers from a high level of interference at the data signals. In contrast, when using DIA, each MS takes into account the interference that it generates to the other MSs. As a result, the overall level of interference in the system is relatively low. Thus, although the MSs do not minimize the own MSE in their best response function, the system benefits from the low level of interference. It is worth noting that although DIA achieves a better sum MSE performance than LBP, LBP requires less CSI than DIA. In LBP each MS needs to know $\sigma_{d,\lambda,\kappa}^2(\mathbf{P})$ and $\sigma_{p,\lambda,\kappa}^2(\mathbf{P})$, whereas in DIA each MS also needs to know the received data power at the BS.

Figure 3 shows the CDF of the individual MSEs of the MSs for the same scenario as considered in Figure 2. The results for $N_r = 10$ show that the individual MSE achieved by the DIA algorithm is distributed within $[-5\mathrm{dB}, 0\mathrm{dB}]$, while that by the LBP algorithm is within $[-25\mathrm{dB}, 0\mathrm{dB}]$. This observation shows that DIA balances the MSE performance of the MSs and achieves better fairness, while LBP allows the MSs in favorable conditions (e.g., close to the cell center) to achieve a lower MSE. This phenomenon can be explained by the difference between LBP and DIA as discussed above. Also, it is interesting
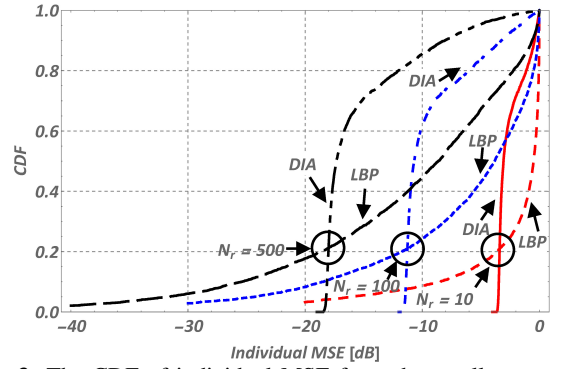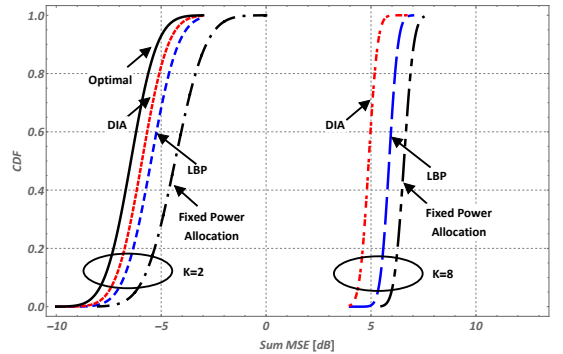
to see that in the scenario in which $N_r = 10$, about 80 percent of the MSs achieve a lower MSE with the DIA algorithm than with the LBP algorithm. This shows that the majority of the MSs benefit from being less greedy. The results for $N_r = 100$ and $N_r = 500$ also show similar behavior as those for $N_r = 10$. Finally, comparing the performance of the algorithms with different number of antennas also shows the benefits of deploying more antennas at the BS.

To benchmark the performance of the algorithms, we also consider a single cell system serving 8 MSs, where there is no pilot contamination and intercell data interference. Figure 4 shows the CDF of the sum MSE of the MSs for the single cell system. Similarly to the three-cell scenario, the DIA outperforms the LBP algorithm, while varying the number of antennas. Comparing Figures 4 and 2 shows that the performance gap between DIA and LBP is larger in the three-cell system than that in the single cell system. For example, when $N_r = 100$, the performance gap between DIA and LBP is at least 3 dB for 40% of the MSs, while it is about 1 dB in the single cell scenario. This shows that setting the data power in a non-selfish way brings more gain to the three-cell system, in which the data interference is more severe than in the single cell system.

In what follows we compare DIA and LBP to the optimal solution and to a fixed power allocation scheme. We obtain the optimal solution by using the optimization solver in Mathematica to solve problem (P1) numerically. The fixed power allocation scheme is motivated by conventional PDPR
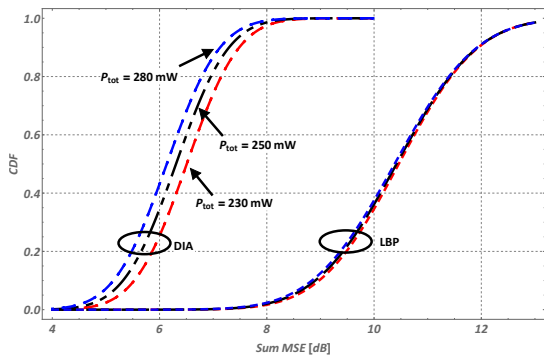
Figure 6: The CDF of sum MSE for a three-cell system, $N_r = 100$, and $P_{tot} = 220$ mW, 250 mW and 280 mW. DIA achieves better performance with higher P_{tot}, whereas LBP is less sensitive to P_{tot}.

Figure 7: The CDF of individual data power for a three-cell system, with $N_r = 10, 100$, and 500. DIA has a larger spread of the data power across the MSs than LBP.

Table III: Average pilot and data power levels (mW)

	DIA		LBP	
	$\tau_d \bar{P}_{\lambda,\kappa}$	$\tau_p \bar{P}_{\lambda,\kappa}^{(p)}$	$\tau_d \bar{P}_{\lambda,\kappa}$	$\tau_p \bar{P}_{\lambda,\kappa}^{(p)}$
Single Cell	113.002	136.978	199.369	50.631
Three Cells	111.940	138.060	198.524	51.476

settings in wireless networks. As an example, in the uplink of 3GPP LTE systems 1 out of 7 OFDM symbols are used for pilot signals, and the rest OFDM symbols are used for data transmission. In accordance with this, in the fixed power allocation scheme we allocate $\frac{1}{7}$ of the total power budget P_{tot} to the pilot symbols of each MS, and allocate the rest of P_{tot} to the data symbols. Figure 5 shows the CDF of sum MSE for a three-cell system with MSs placed at the cell edge, $K \in \{2, 8\}$, and $N_r = 100$. When $K = 2$ DIA performs close to the optimal solution, with a performance gap of about 0.5 dB (due to the complexity of the MSE expression, we were unable to compute an optimal solution for $K > 2$). The results also show that DIA and LBP outperform the fixed power allocation for both values of K, as DIA and LBP allow MSs to adapt their data power with respect to noise and interference.

Furthermore, the scenarios in Figure 5 allow us to investigate the impact of the location of the MSs on the MSE performance. Opposite to intuition, the results for $K = 8$ and $N_r = 100$ in Figures 4 and 5 show that DIA and LBP achieve lower sum MSE when MSs are placed at the cell edge. This is because in interference-limited systems, the MS in the cell center generates higher received power at the serving BS, than the received power from a cell-edge MS. This high received power from a cell center MS at the BS corresponds to a high MU-MIMO interference to the simultaneously served MSs, and thus systems with only edge MSs benefit from a relatively low level of data interference, which compensates the relatively high pathloss of the edge MSs.

To investigate the impact of the total power budget P_{tot} on the MSE performance, in Figure 6 we compare the CDF of sum MSE of a three-cell system for $P_{tot} = 220$ mW, 250 mW and 280 mW, with $N_r = 100$. The figure shows that the sum MSE of DIA decreases as P_{tot} increases, while increasing P_{tot} from 220 mW to 280 mW results in limited improvement for LBP. This can be explained as follows. A higher P_{tot} can benefit a MS by increasing the received pilot and data signal strengths, but also harms the other MSs by higher interference. Compared to LBP, MSs in DIA can benefit more from the increased P_{tot}, as in DIA each MS takes into account the data interference that it generates to the other MSs.
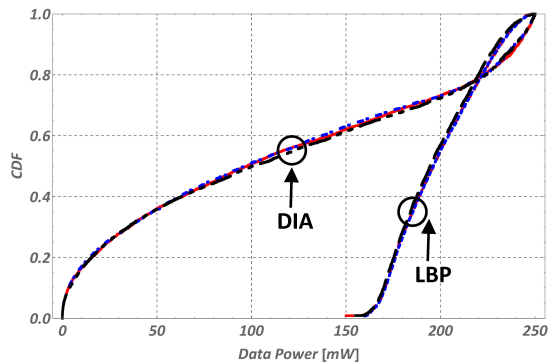
C. PDPR Performance

Figure 7 shows the CDF of the individual data power of the MSs for the same scenario as considered in Figure 2. The results show that in general, DIA has a larger spread of the data power across the MSs than LBP. This is because the DIA algorithm sets very low data power to the MSs with good channel conditions, while it sets high data power to MSs with poor channel conditions. Furthermore, note that the curves for the same algorithm with different number of antennas are very close to each other. This is because DIA only considers the data interference, and the data power is therefore independent of the number of antennas. Similarly, the best response (11) of LBP is also independent of N_r.

To compare the data power setting of DIA and LBP in single cell and three-cell systems, Table III shows the average pilot and data power level of those two algorithms with $N_r = 100$. The table indicates that on average, DIA allocates a higher portion of the power budget to pilot symbols, while LBP allocates higher power levels to data symbols. We can also see that both algorithms allocate more power to pilot symbols in the three-cell scenario. This is because for the three-cell scenario DIA reduces the data power level to mitigate inter-cell data interference, and LBP also increases the pilot power level in response to pilot contamination.

D. Convergence

Figure 8 shows the average number of iterations to convergence as a function of the number of MSs per cell for systems with $1, 2$ and 3 cells, with $N_r = 500$. The confidence intervals of the results are shown at the 95% confidence level. The results show that the average number of iterations for DIA increases linearly as the number of cells or MSs increases. At the same time, the number of iterations for LBP also increases linearly as the number of cells increases, however, the number of iterations for LBP is not sensitive to the number of MSs when $K \geq 3$. The observations show that both LBP and DIA scale well when
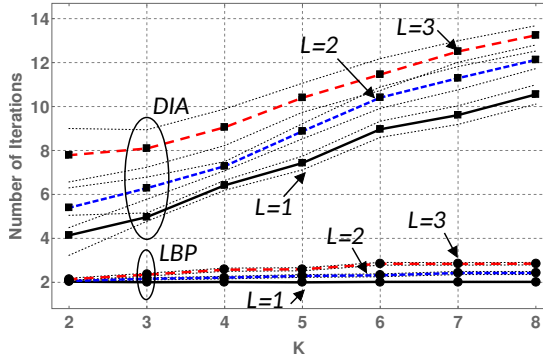
Figure 8: The average number of iterations for convergence for $L = 1, 2,$ and 3 with $N_r = 500$. LBP converges faster than DIA.

the number of cells and MSs increases. It is interesting to see that LBP converges much faster than DIA. For example, for a three-cell system with 8 MSs, LBP converges in average in about 3 iterations, while DIA converges in about 13 iterations. This observation allows to trade off the convergence speed for the MSE performance by deploying DIA or LBP. Finally, recall that in each iteration the execution time of DIA and LBP is independent of the number of cells and MSs, and thus the execution times of DIA and LBP are proportional to the number of iterations for convergence.

IX. CONCLUSIONS

In this paper we considered the uplink of a multi-cell MU-MIMO system, where each MS divides its total power budget between transmitting pilot and data symbols. In this system, the coexistence of pilot contamination and data interference makes the PDPR setting challenging. Furthermore, we argued that due to deploying large scale antenna systems, decentralized PDPR setting schemes are desirable. To this end, we derived a closed form MSE expression for multi-cell MU-MIMO systems, and showed that there exists a unique data power setting for each MS to minimize its own MSE, when the data power setting of all the other MSs is fixed. Based on these results, we modeled the PDPR setting as a non-cooperative game $\mathcal{G}_1$, that allows each MS to minimize its own MSE by setting its data power. We proposed the decentralized LBP algorithm to compute the Nash equilibrium of $\mathcal{G}_1$. Due to the selfish behaviors of the MSs in $\mathcal{G}_1$, the sum MSE performance of the system suffers from a relatively high level of data interference. Motivated by this observation, we further modeled the PDPR setting problem as a game $\mathcal{G}_2$, where the MSs are aware of the data interference in the system. We proposed the decentralized DIA algorithm to compute a data power allocation, and proved that it converges to a Nash equilibrium of $\mathcal{G}_2$. Simulation results showed that the DIA algorithm provides better fairness, while the LBP algorithm allows the MSs with good channel condition to achieve lower MSE.

APPENDIX A
PROOF OF PROPOSITION 1

Following the definition of MSE in (8), we obtain the MSE of the estimated data symbols of the tagged MS (λ, κ) by using the receiver $\mathbf{G}_{\lambda,\kappa}$ as follows,

$$
\begin{aligned}
\text{MSE}&_{\lambda,\kappa}(\mathbf{G}_{\lambda,\kappa}, \mathbf{h}_{1,1,1}, \ldots, \mathbf{h}_{\lambda,L,K}) \\
&= \mathbb{E}_{x,\mathbf{n}_d} \left| \left(\mathbf{G}_{\lambda,\kappa} \alpha_{\lambda,\lambda,\kappa} \mathbf{h}_{\lambda,\lambda,\kappa} \sqrt{P_{\lambda,\kappa}} - 1 \right) x_{\lambda,\kappa} \right|^2 \\
&\quad + \sum_{k \neq \kappa}^{K} P_{\lambda,k} \mathbb{E}_{x,\mathbf{n}_d} \left| \mathbf{G}_{\lambda,\kappa} \alpha_{\lambda,\lambda,k} \mathbf{h}_{\lambda,\lambda,k} x_{\lambda,k} \right|^2 \\
&\quad + \sum_{l \neq \lambda}^{L} \sum_{k}^{K} P_{l,k} \mathbb{E}_{x,\mathbf{n}_d} \left| \mathbf{G}_{\lambda,\kappa} \alpha_{\lambda,l,k} \mathbf{h}_{\lambda,l,k} x_{l,k} \right|^2 \\
&\quad + \mathbb{E}_{x,\mathbf{n}_d} |\mathbf{G}_{\lambda,\kappa} \mathbf{n}_d|^2. \quad (25)
\end{aligned}
$$

By utilizing that $\mathbb{E}\{x_{\lambda,\kappa} x_{\lambda,\kappa}^*\} = 1$ and $\mathbb{E}\{\mathbf{n}_d \mathbf{n}_d *\} = \sigma_d^2 \mathbf{I}$, we obtain

$$
\begin{aligned}
\text{MSE}&_{\lambda,\kappa}(\mathbf{G}_{\lambda,\kappa}, \mathbf{h}_{1,1,1}, \ldots, \mathbf{h}_{\lambda,L,K}) \\
&= \left| \left(\mathbf{G}_{\lambda,\kappa} \alpha_{\lambda,\lambda,\kappa} \mathbf{h}_{\lambda,\lambda,\kappa} \sqrt{P_{\lambda,\kappa}} - 1 \right) \right|^2 \\
&\quad + \sum_{k \neq \kappa}^{K} P_{\lambda,k} |\mathbf{G}_{\lambda,\kappa} \alpha_{\lambda,\lambda,k} \mathbf{h}_{\lambda,\lambda,k}|^2 + \\
&\quad + \sum_{l \neq \lambda}^{L} \sum_{k}^{K} P_{l,k} |\mathbf{G}_{\lambda,\kappa} \alpha_{\lambda,l,k} \mathbf{h}_{\lambda,l,k}|^2 + \sigma_d^2 \mathbf{G}_{\lambda,\kappa} \mathbf{G}_{\lambda,\kappa}^H. \quad (26)
\end{aligned}
$$

Assuming perfect CSI at the BS λ, i.e., $\mathbf{h}_{\lambda,\lambda,\kappa}$ is known, the MSE of the estimated data symbols of the tagged MS (λ, κ) by using the receiver $\mathbf{G}_{\lambda,\kappa}$ is

$$
\begin{aligned}
\text{MSE}&_{\lambda,\kappa}(\mathbf{G}_{\lambda,\kappa}, \mathbf{h}_{\lambda,\lambda,\kappa}) \\
&= \mathbb{E}_{\mathbf{h}_{1,1,1},\ldots,\mathbf{h}_{\lambda,L,K}} \{ \text{MSE}_{\lambda,\kappa}(\mathbf{G}_{\lambda,\kappa}, \mathbf{h}_{1,1,1}, \ldots, \mathbf{h}_{\lambda,L,K}) \} \\
&= \alpha_{\lambda,\lambda,\kappa}^2 P_{\lambda,\kappa} \mathbf{G}_{\lambda,\kappa} \mathbf{h}_{\lambda,\lambda,\kappa} \mathbf{h}_{\lambda,\lambda,\kappa}^H \mathbf{G}_{\lambda,\kappa}^H \\
&\quad - \alpha_{\lambda,\lambda,\kappa} \sqrt{P_{\lambda,\kappa}} \left(\mathbf{G}_{\lambda,\kappa} \mathbf{h}_{\lambda,\lambda,\kappa} + \mathbf{h}_{\lambda,\lambda,\kappa}^H \mathbf{G}_{\lambda,\kappa}^H \right) \\
&\quad + \sum_{l \neq \lambda}^{L} \sum_{k}^{K} \alpha_{\lambda,l,k}^2 P_{l,k} \mathbf{G}_{\lambda,\kappa} \mathbf{C}_{\lambda,l,k} \mathbf{G}_{\lambda,\kappa}^H \\
&\quad + \sum_{k \neq \kappa}^{K} \alpha_{\lambda,\lambda,k}^2 P_{\lambda,k} \mathbf{G}_{\lambda,\kappa} \mathbf{C}_{\lambda,\lambda,k} \mathbf{G}_{\lambda,\kappa}^H + \sigma_d^2 \mathbf{G}_{\lambda,\kappa} \mathbf{G}_{\lambda,\kappa}^H + 1. \quad (27)
\end{aligned}
$$

By applying the result that $(\mathbf{h}|\hat{\mathbf{h}}) \sim \mathcal{CN}(\mathbf{D}\hat{\mathbf{h}}, \mathbf{Q})$, the MSE of the estimated data symbols of the tagged MS (λ, κ) as a function of the estimated channel $\hat{\mathbf{h}}_{\lambda,\lambda,\kappa}$ is

$$
\begin{aligned}
\text{MSE}&_{\lambda,\kappa}(\mathbf{G}_{\lambda,\kappa}, \hat{\mathbf{h}}_{\lambda,\lambda,\kappa}) \\
&= \mathbb{E}_{\mathbf{h}_{\lambda,\lambda,\kappa}|\hat{\mathbf{h}}_{\lambda,\lambda,\kappa}} \{ \text{MSE}_{\lambda,\kappa}(\mathbf{G}_{\lambda,\kappa}, \mathbf{h}_{\lambda,\lambda,\kappa}) \} \\
&= \alpha_{\lambda,\lambda,\kappa}^2 P_{\lambda,\kappa} \mathbf{G}_{\lambda,\kappa} \left(\mathbf{D}_{\lambda,\lambda,\kappa} \hat{\mathbf{h}}_{\lambda,\lambda,\kappa} \hat{\mathbf{h}}_{\lambda,\lambda,\kappa}^H \mathbf{D}_{\lambda,\lambda,\kappa}^H + \mathbf{Q}_{\lambda,\lambda,\kappa} \right) \mathbf{G}_{\lambda,\kappa}^H \\
&\quad - \alpha_{\lambda,\lambda,\kappa} \sqrt{P_{\lambda,\kappa}} \left(\mathbf{G}_{\lambda,\kappa} \mathbf{D}_{\lambda,\lambda,\kappa} \hat{\mathbf{h}}_{\lambda,\lambda,\kappa} + \hat{\mathbf{h}}_{\lambda,\lambda,\kappa}^H \mathbf{D}_{\lambda,\lambda,\kappa}^H \mathbf{G}_{\lambda,\kappa}^H \right) \\
&\quad + \sum_{l \neq \lambda}^{L} \sum_{k}^{K} \alpha_{\lambda,l,k}^2 P_{l,k} \mathbf{G}_{\lambda,\kappa} \mathbf{C}_{\lambda,l,k} \mathbf{G}_{\lambda,\kappa}^H \\
&\quad + \sum_{k \neq \kappa}^{K} \alpha_{\lambda,\lambda,k}^2 P_{\lambda,k} \mathbf{G}_{\lambda,\kappa} \mathbf{C}_{\lambda,\lambda,k} \mathbf{G}_{\lambda,\kappa}^H + \sigma_d^2 \mathbf{G}_{\lambda,\kappa} \mathbf{G}_{\lambda,\kappa}^H + 1. \quad (28)
\end{aligned}
$$

Since we assume the proper antenna spacing, substituting $\mathbf{G}_{\lambda,\kappa} = g_{\lambda,\kappa} \cdot \hat{\mathbf{h}}_{\lambda,\lambda,\kappa}^H$, $\mathbf{R}_{\lambda,\lambda,\kappa}(\mathbf{P}) = r_{\lambda,\lambda,\kappa}(\mathbf{P}) \cdot \mathbf{I}$, $\mathbf{D}_{\lambda,\lambda,\kappa}(\mathbf{P}) =$

$d_{\lambda,\lambda,\kappa}(\mathbf{P}) \cdot \mathbf{I}$, $\mathbf{Q}_{\lambda,\lambda,\kappa}(\mathbf{P}) = q_{\lambda,\lambda,\kappa}(\mathbf{P}) \cdot \mathbf{I}$ into (28) yields

$$\text{MSE}_{\lambda,\kappa}(\mathbf{G}_{\lambda,\kappa}, \hat{\mathbf{h}}_{\lambda,\lambda,\kappa}) \tag{29}$$
$$= 1 - 2\alpha_{\lambda,\lambda,\kappa}\sqrt{P_{\lambda,\kappa}} g_{\lambda,\kappa} d_{\lambda,\lambda,\kappa} ||\hat{\mathbf{h}}_{\lambda,\lambda,\kappa}||^2$$
$$+ g_{\lambda,\kappa}^2 \left(\alpha_{\lambda,\lambda,\kappa}^2 P_{\lambda,\kappa} d_{\lambda,\lambda,\kappa}^2 ||\hat{\mathbf{h}}_{\lambda,\lambda,\kappa}||^4 \right.$$
$$\left. + \left(\alpha_{\lambda,\lambda,\kappa}^2 P_{\lambda,\kappa} q_{\lambda,\lambda,\kappa} + \sigma_{\lambda,\kappa}^2(\mathbf{P}_{-(\lambda,\kappa)}) \right) ||\hat{\mathbf{h}}_{\lambda,\lambda,\kappa}||^2 \right).$$

For convenience, we define

$$T_1 = g_{\lambda,\kappa}^2\, \alpha_{\lambda,\lambda,\kappa}^2 P_{\lambda,\kappa} d_{\lambda,\lambda,\kappa}^2 ||\hat{\mathbf{h}}_{\lambda,\lambda,\kappa}||^4,$$
$$T_2 = g_{\lambda,\kappa}^2 \left(\alpha_{\lambda,\lambda,\kappa}^2 P_{\lambda,\kappa} q_{\lambda,\lambda,\kappa} + \sigma_{\lambda,\kappa}^2(\mathbf{P}_{-(\lambda,\kappa)}) \right) ||\hat{\mathbf{h}}_{\lambda,\lambda,\kappa}||^2,$$
$$T_3 = 2\alpha_{\lambda,\lambda,\kappa}\sqrt{P_{\lambda,\kappa}} g_{\lambda,\kappa} d_{\lambda,\lambda,\kappa} ||\hat{\mathbf{h}}_{\lambda,\lambda,\kappa}||^2, \tag{30}$$

and therefore $\text{MSE}_{\lambda,\kappa}(\mathbf{G}_{\lambda,\kappa}, \hat{\mathbf{h}}_{\lambda,\lambda,\kappa}) = T1 + T2 - T3 + 1$.

In what follows, we derive the unconditional MSE of the estimated data symbols of the tagged MS (λ, κ) for multi-cell MU-MIMO with pilot contamination, and the proof is an extension of the proof of MSE in single cell without pilot contamination in [Proposition 1, Lemma 2, [18]]. We denote by $\text{MSE}_{\lambda,\kappa}(\mathbf{P})$ the unconditional MSE of the estimated data symbols of the tagged MS (λ, κ), which emphasizes fact that the unconditional MSE is a function of the data power of all MSs.

We define $s_{\lambda,\lambda,\kappa} = d_{\lambda,\lambda,\kappa}^2 P_{\lambda,\lambda,\kappa}$ and $b_{\lambda,\lambda,\kappa} = q_{\lambda,\lambda,\kappa}^2 P_{\lambda,\lambda,\kappa} + \sigma_{\lambda,\kappa}^2$, and drop the indices of $s_{\lambda,\lambda,\kappa}$, $b_{\lambda,\lambda,\kappa}$, $r_{\lambda,\lambda,\kappa}$ in the following proof for simplicity.

Recognizing that $||\hat{\mathbf{h}}_{\lambda,\lambda,\kappa}||^2$ follows the Gama distribution, the density function of $||\hat{\mathbf{h}}_{\lambda,\lambda,\kappa}||^2$ is

$$f_{||\hat{\mathbf{h}}_{\lambda,\lambda,\kappa}||^2}(x) = \frac{r^{-N_r} x^{N_r-1} e^{-\frac{x}{r}}}{(N_r - 1)!}, x > 0. \tag{31}$$

To obtain $\text{MSE}_{\lambda,\kappa}(\mathbf{P})$, we take the average of $\text{MSE}_{\lambda,\kappa}(\mathbf{G}_{\lambda,\kappa}, \hat{\mathbf{h}}_{\lambda,\lambda,\kappa})$ by using the following integrals,

$$\int_{x=0}^{\infty} T_1 f_{||\hat{\mathbf{h}}_{\lambda,\lambda,\kappa}||^2}(x) dx \tag{32}$$
$$= N_r \left(e^{\frac{b}{sr}} \left(b + (1 + N_r) sr \right) E_{in}\left(1 + N_r, \frac{b}{sr}\right) - sr \right) \Big/ (sr),$$

$$\int_{x=0}^{\infty} T_2 f_{||\hat{\mathbf{h}}_{\lambda,\lambda,\kappa}||^2}(x) dx \tag{33}$$
$$= b \left(e^{\frac{b}{sr}} \left(b + N_r sr \right) E_{in}\left(N_r, \frac{b}{sr}\right) - sr \right) \Big/ (s^2 r^2),$$

$$\int_{x=0}^{\infty} T_3 f_{||\hat{\mathbf{h}}_{\lambda,\lambda,\kappa}||^2}(x) dx = 2 \cdot e^{\frac{b}{sr}} N_r E_{in}\left(N_r, \frac{b}{sr}\right), \tag{34}$$

where $E_{in}(n, z) \triangleq \int_1^{\infty} e^{-zt}/t^n dt$ is the standard exponential integral function. Therefore, the unconditional MSE is

$$\text{MSE}_{\lambda,\kappa}(\mathbf{P}) = \frac{N_r \left(e^{\frac{b}{sr}} \left(b + (1 + N_r) sr \right) E_{in}\left(1 + N_r, \frac{b}{sr}\right) - sr \right)}{sr}$$
$$+ \frac{b \left(e^{\frac{b}{sr}} \left(b + N_r sr \right) E_{in}\left(N_r, \frac{b}{sr}\right) - sr \right)}{s^2 r^2}$$
$$- 2 \cdot e^{\frac{b}{sr}} N_r E_{in}\left(N_r, \frac{b}{sr}\right) + 1. \tag{35}$$

Now we rewrite the MSE expression in (35) by making use of the following recursive relation ([8.19.12, [36]]),

$$\mu_{\lambda,\kappa} E_{in}(N_r, \mu_{\lambda,\kappa}) + N_r E_{in}(N_r + 1, \mu_{\lambda,\kappa}) = e^{-\mu_{\lambda,\kappa}}. \tag{36}$$

Define $\mu_{\lambda,\kappa} = \frac{b}{rs}$, and we obtain (10) by substituting b, r, and s into $\mu_{\lambda,\kappa}$. Substituting $\mu_{\lambda,\kappa}$ in (10) into (36), and rearranging, we obtain (9).

APPENDIX B
PROOF OF LEMMA 1

The first derivative of the $\text{MSE}_{\lambda,\kappa}(\mathbf{P})$ with respect to $P_{\lambda,\kappa}$ is

$$\frac{\partial \text{MSE}_{\lambda,\kappa}(\mathbf{P})}{\partial P_{\lambda,\kappa}} = \frac{\partial \text{MSE}_{\lambda,\kappa}(\mathbf{P})}{\partial \mu_{\lambda,\kappa}} \cdot \frac{\partial \mu_{\lambda,\kappa}(\mathbf{P})}{\partial P_{\lambda,\kappa}}. \tag{37}$$

From [18, Appendix III], $\frac{\partial \text{MSE}_{\lambda,\kappa}(\mathbf{P})}{\partial \mu_{\lambda,\kappa}}$ is positive $\forall \mu_{\lambda,\kappa}(\mathbf{P}) > 0$.

According to the system model, when $P_{\lambda,\kappa} \in \mathcal{P}_d$, $P_{tot} - P_{\lambda,\kappa}\tau_d > 0$ and thus $\mu_{\lambda,\kappa}(\mathbf{P})$ is always positive. Thus the sign of $\frac{\partial \text{MSE}_{\lambda,\kappa}(\mathbf{P})}{\partial \mu_{\lambda,\kappa}}$ in (37) only depends on the sign of $\frac{\partial \mu_{\lambda,\kappa}(\mathbf{P})}{\partial P_{\lambda,\kappa}}$. Further investigation shows $\frac{\partial \mu_{\lambda,\kappa}(\mathbf{P})}{\partial P_{\lambda,\kappa}} = 0$ has unique solution $P_{\lambda,\kappa}^*$ in $\mathcal{P}_d$, and $\frac{\partial \mu_{\lambda,\kappa}(\mathbf{P})}{\partial P_{\lambda,\kappa}} \frac{\partial \text{MSE}_{\lambda,\kappa}(\mathbf{P})}{\partial P_{\lambda,\kappa}} < 0$ for $\forall P_{\lambda,\kappa} \in (0, P_{\lambda,\kappa}^*]$, and $\frac{\partial \mu_{\lambda,\kappa}(\mathbf{P})}{\partial P_{\lambda,\kappa}} \frac{\partial \text{MSE}_{\lambda,\kappa}(\mathbf{P})}{\partial P_{\lambda,\kappa}} > 0$ for $\forall P_{\lambda,\kappa} \in [P_{\lambda,\kappa}^*, \frac{P_{tot}}{\tau_d})$. Therefore, $P_{\lambda,\kappa}^*$, as shown in (11), is the unique minimizer of $\text{MSE}_{\lambda,\kappa}(\mathbf{P})$.

APPENDIX C
PROOF OF LEMMA 2

Taking the first derivative of $P_{\lambda,\kappa}^\star(\mathbf{P}_{-(\lambda,\kappa)})$ with respect to the data power $P_{l,j}$ of MS j in cell l we obtain

$$\frac{\partial P_{\lambda,\kappa}^\star(\mathbf{P}_{-(\lambda,\kappa)})}{\partial P_{l,j}} = c_{\lambda,\lambda,\kappa} P_{tot}^2 \alpha_{\lambda,l,j} \tau_d \cdot$$
$$\frac{\left(\frac{V\alpha_{\lambda,\lambda,\kappa}^2 \tau_d \tau_p}{U^2} + \frac{W}{\left(\left(\sigma_{\lambda,\kappa}^2(\mathbf{P}_{-(\lambda,\kappa)}) - P_{l,j}\alpha_{\lambda,l,j}^2 c_{\lambda,l,j} \right) + \alpha_{\lambda,l,j} P_{l,j} \right)^2} \right)}{2W^2 \sqrt{\frac{V\tau_d}{W}} \left(\tau_d + \sqrt{\frac{V\tau_d}{W}} \right)^2}, \tag{38}$$

where

$$U = \alpha_{\lambda,l,j} \left(P_{tot} - \tau_d P_{l,j} \right) +$$
$$\left(\sigma_{\text{pc},\lambda,\kappa}^2(\mathbf{P}_{-(\lambda,\kappa)}) - \frac{(P_{tot} - \tau_d P_{l,j})}{\tau_p} \alpha_{\lambda,l,j}^2 c_{\lambda,l,j} \right) \tau_p, \tag{39}$$

$$V = \tau_d + \frac{c_{\lambda,\lambda,\kappa} P_{tot}}{\left(\sigma_{\lambda,\kappa}^2(\mathbf{P}_{-(\lambda,\kappa)}) - P_{l,j}\alpha_{\lambda,l,j}^2 c_{\lambda,l,j} \right) + \alpha_{\lambda,l,j} P_{l,j}}, \tag{40}$$

and

$$W = 1 + \frac{c_{\lambda,\lambda,\kappa} P_{tot} \alpha_{\lambda,\lambda,\kappa}^2 \tau_p}{U}. \tag{41}$$

Since $\frac{\partial P_{\lambda,\kappa}^\star(\mathbf{P}_{-(\lambda,\kappa)})}{\partial P_{l,j}}$ is positive, the best response function of MS κ in cell λ is an increasing function of the data power of MS j in cell l.

APPENDIX D
PROOF OF LEMMA 3

Since $\sigma_{\mathrm{pc},\lambda,\kappa}^2(\mathbf{P}_{-(\lambda,\kappa)}) > 0$ and $\sigma_{\lambda,\kappa}^2(\mathbf{P}_{-(\lambda,\kappa)}) > 0$ holds for any $\mathbf{0} \leq \mathbf{P}_{(-\lambda,\kappa)} \leq \frac{P_{tot}}{\tau_d}\mathbf{e}$, and thus $M(\mathbf{P}_{-(\lambda,\kappa)}) > 0$. Hence, $0 < \underline{P_{\lambda,\kappa}}, \overline{P_{\lambda,\kappa}} < \frac{P_{tot}}{\tau_d}$, and we prove the Lemma.

APPENDIX E
PROOF OF LEMMA 4

From [18, Appendix III] $\frac{\partial \mathrm{MSE}_{\lambda,\kappa}(\mathbf{P})}{\partial P_{\lambda,\kappa}}$ is a product of continuous functions on $[\underline{P_{\lambda,\kappa}}, \overline{P_{\lambda,\kappa}}]$, and thus $\frac{\partial \mathrm{MSE}_{\lambda,\kappa}(\mathbf{P})}{\partial P_{\lambda,\kappa}}$ is a continuous function on $[\underline{P_{\lambda,\kappa}}, \overline{P_{\lambda,\kappa}}]$. Therefore, $\frac{\partial \mathrm{MSE}_{\lambda,\kappa}(\mathbf{P})}{\partial P_{\lambda,\kappa}}$ is bounded on the closed interval $[\underline{P_{\lambda,\kappa}}, \overline{P_{\lambda,\kappa}}]$, and $\max\{|\frac{\partial \mathrm{MSE}_{\lambda,\kappa}(\mathbf{P})}{\partial P_{\lambda,\kappa}}|\}$ exists. [32, Chapter 6.2]

APPENDIX F
APPENDIX: PROOF OF LEMMA 5

According to the proof of Theorem 2 in [37], the condition that $\mathbf{f}(\mathbf{P})$ is a contraction mapping in $\mathcal{P}_d^{1 \times KL}$ is

$$||\mathbf{F}(\mathbf{P})||_1 = \max_j \sum_{i=1}^K |\mathbf{F}(\mathbf{P})_{ij}| \leq \eta, \tag{42}$$

where $\eta < 1$ is a number close to one. (42) can be reformulated as

$$\sum_{l=1}^L \sum_{k=1}^K L \frac{\partial P_{\lambda,\kappa}^\star(\mathbf{P}_{-(\lambda,\kappa)})}{\partial P_{l,k}} \leq \eta < 1, \quad \forall \lambda, \kappa. \tag{43}$$

APPENDIX G
PROOF OF LEMMA 7

We consider two arbitrary data powers $P_{\lambda,\kappa}$, $P_{\lambda,\kappa}' \in \mathcal{P}_d$ for MS (λ, κ). When MS (λ, κ) changes its data power from $P_{\lambda,\kappa}$ to $P_{\lambda,\kappa}'$, the change of its cost function is

$$\Delta u_{\lambda,\kappa} = u_{\lambda,\kappa}(P_{\lambda,\kappa}, \mathbf{P}_{-(\lambda,\kappa)}) - u_{\lambda,\kappa}(P_{\lambda,\kappa}', \mathbf{P}_{-(\lambda,\kappa)}),$$

and the change of the function $\Psi(\mathbf{P})$ is

$$\Delta\Psi = \Psi(P_{\lambda,\kappa}, \mathbf{P}_{-(\lambda,\kappa)}) - \Psi(P_{\lambda,\kappa}', \mathbf{P}_{-(\lambda,\kappa)}).$$

According to Definition 2, to prove that $\Psi(\mathbf{P})$ is a potential function of $\mathcal{G}_2$, we only need to prove that $\Delta\Psi = \Delta u_{\lambda,\kappa}$. We rewrite ΔO as

$$\Delta O = \frac{1}{2}\sum_{l=1}^L \sum_{k=1}^K \left(\gamma_{l,k}(P_{\lambda,\kappa}, \mathbf{P}_{-(\lambda,\kappa)}) - \gamma_{l,k}(P_{\lambda,\kappa}', \mathbf{P}_{-(\lambda,\kappa)})\right)$$
$$+ \frac{1}{2}\sum_{l=1}^L \sum_{k=1}^K \left(\theta_{l,k}(P_{\lambda,\kappa}, \mathbf{P}_{-(\lambda,\kappa)}) - \theta_{l,k}(P_{\lambda,\kappa}', \mathbf{P}_{-(\lambda,\kappa)})\right). \tag{44}$$

According to (18), when $l \neq \lambda$ and $k \neq \kappa$ we have

$$\gamma_{l,k}(\mathbf{P}) = \frac{\sum_{m \neq k}^K \alpha_{l,l,m}^2 P_{l,m} + \sum_{i \neq l}^L \sum_m^K \alpha_{l,i,m}^2 P_{i,m}}{\alpha_{l,l,k}^2 P_{l,k}}. \tag{45}$$

Since only the data power of MS (λ, κ) is changed, and therefore for all $l \neq \lambda$ and $k \neq \kappa$,

$$\gamma_{l,k}(P_{\lambda,\kappa}, \mathbf{P}_{-(\lambda,\kappa)}) - \gamma_{l,k}(P_{\lambda,\kappa}', \mathbf{P}_{-(\lambda,\kappa)})$$
$$= \frac{\alpha_{l,\lambda,\kappa}^2 P_{\lambda,\kappa} - \alpha_{l,\lambda,\kappa}^2 P_{\lambda,\kappa}'}{\alpha_{l,l,k}^2 P_{l,k}}. \tag{46}$$

Further, we have

$$\sum_{l=1}^L \sum_{k=1}^K \left(\gamma_{l,k}(P_{\lambda,\kappa}, \mathbf{P}_{-(\lambda,\kappa)}) - \gamma_{l,k}(P_{\lambda,\kappa}', \mathbf{P}_{-(\lambda,\kappa)})\right)$$
$$= \sum_{k \neq \kappa}^K \frac{\alpha_{\lambda,\lambda,\kappa}^2 P_{\lambda,\kappa} - \alpha_{\lambda,\lambda,\kappa}^2 P_{\lambda,\kappa}'}{\alpha_{\lambda,\lambda,k}^2 P_{\lambda,k}}$$
$$+ \sum_{l \neq \lambda}^L \sum_k^K \frac{\alpha_{l,\lambda,\kappa}^2 P_{\lambda,\kappa} - \alpha_{l,\lambda,\kappa}^2 P_{\lambda,\kappa}'}{\alpha_{l,l,k}^2 P_{l,k}}$$
$$+ \left(\gamma_{\lambda,\kappa}(P_{\lambda,\kappa}, \mathbf{P}_{-(\lambda,\kappa)}) - \gamma_{\lambda,\kappa}(P_{\lambda,\kappa}', \mathbf{P}_{-(\lambda,\kappa)})\right)$$
$$= \theta_{\lambda,\kappa}(P_{\lambda,\kappa}, \mathbf{P}_{-(\lambda,\kappa)}) - \theta_{\lambda,\kappa}(P_{\lambda,\kappa}', \mathbf{P}_{-(\lambda,\kappa)}) \tag{47}$$
$$+ \gamma_{\lambda,\kappa}(P_{\lambda,\kappa}, \mathbf{P}_{-(\lambda,\kappa)}) - \gamma_{\lambda,\kappa}(P_{\lambda,\kappa}', \mathbf{P}_{-(\lambda,\kappa)}) = \Delta u_{\lambda,\kappa}.$$

Similarly, when $l \neq \lambda$ and $k \neq \kappa$ we have

$$\theta_{l,k}(P_{\lambda,\kappa}, \mathbf{P}_{-(\lambda,\kappa)})$$
$$= P_{l,k}\left(\sum_{m \neq k}^K \frac{\alpha_{l,l,k}^2}{\alpha_{l,l,m}^2 P_{l,m}} + \sum_{i \neq l}^L \sum_m^K \frac{\alpha_{i,l,k}^2}{\alpha_{i,i,m}^2 P_{i,m}}\right). \tag{48}$$

and since only MS (λ, κ) changes its data power, when $l \neq \lambda$ and $k \neq \kappa$,

$$\theta_{l,k}(P_{\lambda,\kappa}, \mathbf{P}_{-(\lambda,\kappa)}) - \theta_{l,k}(P_{\lambda,\kappa}', \mathbf{P}_{-(\lambda,\kappa)})$$
$$= \frac{\alpha_{\lambda,l,k}^2 P_{l,k}}{\alpha_{\lambda,\lambda,\kappa}^2 P_{\lambda,\kappa}} - \frac{\alpha_{\lambda,l,k}^2 P_{l,k}}{\alpha_{\lambda,\lambda,\kappa}^2 P_{\lambda,\kappa}'}. \tag{49}$$

Therefore,

$$\sum_l^L \sum_k^K \left(\theta_{l,k}(P_{\lambda,\kappa}, \mathbf{P}_{-(\lambda,\kappa)}) - \theta_{l,k}(P_{\lambda,\kappa}', \mathbf{P}_{-(\lambda,\kappa)})\right)$$
$$= \sum_{k \neq \kappa}^K \frac{\alpha_{\lambda,\lambda,k}^2 P_{\lambda,k}}{\alpha_{\lambda,\lambda,\kappa}^2 P_{\lambda,\kappa}} + \sum_{l \neq \lambda}^L \sum_k^K \frac{\alpha_{\lambda,l,k}^2 P_{l,k}}{\alpha_{\lambda,\lambda,\kappa}^2 P_{\lambda,\kappa}} \tag{50}$$

$$- \sum_{k \neq \kappa}^K \frac{\alpha_{\lambda,\lambda,k}^2 P_{\lambda,k}}{\alpha_{\lambda,\lambda,\kappa}^2 P_{\lambda,\kappa}'} - \sum_{l \neq \lambda}^L \sum_k^K \frac{\alpha_{\lambda,l,k}^2 P_{l,k}}{\alpha_{\lambda,\lambda,\kappa}^2 P_{\lambda,\kappa}'}$$
$$+ \theta_{\lambda,\kappa}(P_{\lambda,\kappa}, \mathbf{P}_{-(\lambda,\kappa)}) - \theta_{\lambda,\kappa}(P_{\lambda,\kappa}', \mathbf{P}_{-(\lambda,\kappa)})$$
$$= \gamma_{\lambda,\kappa}(P_{\lambda,\kappa}, \mathbf{P}_{-(\lambda,\kappa)}) - \gamma_{\lambda,\kappa}(P_{\lambda,\kappa}', \mathbf{P}_{-(\lambda,\kappa)}) \tag{51}$$
$$+ \theta_{\lambda,\kappa}(P_{\lambda,\kappa}, \mathbf{P}_{-(\lambda,\kappa)}) - \theta_{\lambda,\kappa}(P_{\lambda,\kappa}', \mathbf{P}_{-(\lambda,\kappa)}) = \Delta u_{\lambda,\kappa}.$$

Substituting (47) and (51) in (44) shows that

$$\Delta\Psi = \frac{1}{2}\Delta u_{\lambda,\kappa} + \frac{1}{2}\Delta u_{\lambda,\kappa} = \Delta u_{\lambda,\kappa}, \tag{52}$$

which proves the lemma.

REFERENCES

[1] S. Sesia, I. Toufik, and M. Baker, *LTE - The UMTS Long Term Evolution: From Theory to Practice*. WILEY, 2nd edition, 2011, ISBN-10: 0470660252.

[2] M. Médard, "The effect upon channel capacity in wireless communications of perfect and imperfect knowledge of the channel," *IEEE Trans. Inf. Theory*, vol. 46, no. 3, pp. 933–946, May 2000.

[3] B. Hassibi and B. M. Hochwald, "How much training is needed in multiple-antenna wireless links ?" *IEEE Trans. Inf. Theory*, vol. 49, no. 4, pp. 951–963, April 2003.

[4] T. Kim and J. G. Andrews, "Optimal pilot-to-data power ratio for MIMO-OFDM," in *Proc. GLOBECOME*, St. Louis, MO, USA, Dec. 2005, pp. 1481–1485.

[5] T. Marzetta, "Noncooperative cellular wireless with unlimited numbers of base station antennas," *IEEE Trans. Wireless Commun.*, vol. 9, no. 11, pp. 3590–3600, 2010.

[6] T. Kim and J. G. Andrews, "Balancing pilot and data power for adaptive MIMO-OFDM systems," in *Proc. GLOBECOM*, San Francisco, CA, USA, Dec 2006.

[7] T. Marzetta, "How much training is needed for multiuser MIMO ?" *Proc. IEEE Asilomar Conf. Signals, Syst. Comput. (ACSSC)*, pp. 359–363, June 2006.

[8] K. Guo, Y. Guo, G. Fodor, and G. Ascheid, "Uplink power control with mmse receiver in multi-cell MU-Massive-MIMO systems," in *Proc. IEEE Int. Conf. Commun. (ICC)*, Jun. 2014, pp. 5184–5190.

[9] X. Li, E. Björnsson, E. G. Larsson, S. Zhou, and J. Wang, "Massive MIMO with multi-cell mmse processing: Exploiting all pilots for interference suppression," *arXiv:1505.03682v2 [cs.IT]*, May 2015.

[10] H. Ahmadi, A. Farhang, N. Marchetti, and A. MacKenzie, "A game theoretic approach for pilot contamination avoidance in massive MIMO," *IEEE Wireless Commun. Lett.*, vol. 5, no. 1, pp. 12–15, February 2016.

[11] B. Gopalakrishnan and N. Jindal, "An analysis of pilot contamination on multi-user mimo cellular systems with many antennas," in *IEEE International Workshop on Signal Processing Advances in Wireless Communications*. IEEE, 2011, pp. 381–385.

[12] C. P. Sukumar and R. M. M. Eltawil, "Joint power loading of data and pilots in OFDM using imperfect channel state information at the transmitter," in *Proc. GLOBECOM*, Nov. 2008, pp. 1–5.

[13] N. Jindal and A. Lozano, "A unified treatment of optimum pilot overhear in multipath fading channels," *IEEE Trans. Commun.*, vol. 58, no. 10, pp. 2939–2948, October 2010.

[14] K. Min, M. Jung, T. Kim, Y. Kim, J. Lee, and S. Choi, "Pilot power ratio for uplink sum-rate maximization in zero-forcing based MU-MIMO systems with large number of antennas," in *Proc. IEEE Veh. Technol. Conf. (VTC-Fall)*, 2-5 September 2013, pp. 1–5.

[15] K. T. Truong, A. Lozano, and R. W. H. Jr., "Optimal training in continuous block-fading massive MIMO systems," *Proc. 20th Eur. Wireless*, May 2014.

[16] N. Sun and J. Wu, "Maximizing spectral efficiency for high mobility systems with imperfect channel state information," *IEEE Trans. Wireless Commun.*, vol. 13, no. 3, pp. 1462–1470, March 2014.

[17] K. Guo, Y. Guo, and G. Ascheid, "Energy-efficient uplink power allocation in Multi-Cell MU-Massive-MIMO systems," in *Proc. Eur. Wireless*, Budapest, Hungary, May 2015, pp. 1–5.

[18] G. Fodor, P. D. Marco, and M. Telek, "On the Impact of Antenna Correlation and CSI Errors on the Pilot-to-Data Power Ratio," *IEEE Trans. Commun.*, vol. 64, no. 6, pp. 2622 – 2633, April 2016.

[19] M. Ding and S. D. Blostein, "Relation between joint optimizations for multiuser MIMO uplink and downlink with imperfect CSI," in *Proc. IEEE Int. Conf. Acoust., Speech, Signal Process. (ICASSP)*, Las vegas, NV, USA, March 31-April 4 2008, pp. 3149 – 3152.

[20] J. Kron, D. Persson, M. Skoglund, and E. G. Larsson, "Closed-form Sum-MSE minimization for the two-user gaussian MIMO broadcast channel," *IEEE Commun. Lett.*, vol. 15, no. 9, pp. 950–952, Sep. 2011.

[21] J. Wang, M. Bengtsson, B. Ottersten, and D. Palomar, "Robust MIMO precoding for several classes of channel uncertainty," *IEEE Trans. Signal Process.*, vol. 61, no. 12, pp. 3056–3070, April 2013.

[22] H. Yin, D. Gesbert, M. Filippou, and Y. Liu, "A Coordinated Approach to Channel Estimation in Large-Scale Multiple-Antenna Systems," *IEEE J. Sel. Areas Commun.*, vol. 31, no. 2, pp. 264–273, February 2013.

[23] Y. Shi, J. Wang, K. B. Letaief, and R. K. Mallik, "A game-theoretic approach for distributed power control in interference relay channels," *IEEE Trans. Wireless Commun.*, vol. 8, no. 6, pp. 3151–3161, 2009.

[24] L. Song, Z. Han, Z. Zhang, and B. Jiao, "Non-cooperative feedback-rate control game for channel state information in wireless networks," *IEEE J. Sel. Areas Commun.*, vol. 30, no. 1, pp. 188–197, 2012.

[25] J. Wang, W. Guan, Y. Huang, R. Schober, and X. You, "Distributed optimization of hierarchical small cell networks: A gnep framework," *IEEE J. Sel. Areas Commun.*, vol. 35, no. 2, pp. 249–264, Feb. 2017.

[26] I. Stupia, L. Sanguinetti, G. Bacci, and L. Vandendorpe, "Power control in networks with heterogeneous users: A quasi-variational inequality approach," *IEEE Trans. Signal Process.*, vol. 63, no. 21, pp. 5691–5705, Nov. 2015.

[27] V. Pacifici and G. Dán, "Convergence in player-specific graphical resource allocation games," *IEEE J. Sel. Areas Commun.*, vol. 30, no. 11, pp. 2190–2199, Dec. 2012.

[28] G. Fodor, P. D. Marco, and M. Telek, "Performance analysis of block and comb type channel estimation for massive MIMO systems," in *First International Conference on 5G for Ubiquitous Connectivity (5GU)*, Nov. 2014, pp. 62–69.

[29] ——, "On minimizing the MSE in the presence of channel information errors," *IEEE Commun. Lett.*, vol. 19, no. 9, pp. 1604 – 1607, September 2015.

[30] V.-D. Nguyen, H. V. Nguyen, Y. Shin, W.-C. Lee, and O.-S. Shin, "Channel estimation and data detection for multicell massive MIMO systems in correlated channels," *Wireless Pers. Commun.*, no. 86, pp. 1857–1877, December 2016.

[31] S. Boyd and L. Vandenberghe, *Convex optimization*, 1st ed. Cambridge University Press, 2004.

[32] L. Rade and B. Westergren, *Mathematics handbook for science and engineering*. Germany: Springer Science & Business Media, 2013.

[33] A. B. MacKenzie and L. A. DaSilva, "Game theory for wireless engineers," *Synthesis Lectures on Communications*, vol. 1, no. 1, pp. 1–86, 2006.

[34] D. Monderer and L. S. Shapley, "Potential games," *Games and economic behavior*, vol. 14, no. 1, pp. 124–143, 1996.

[35] Q. D. La, Y. H. Chew, and B.-H. Soong, *Potential game theory: applications in radio resource allocation*. Springer, 2016.

[36] F. W. Olver, D. W. Lozier, R. F. Boisvert, and C. W. Clark, Eds., *NIST Handbook of Mathematical Functions*, 1st ed. New York, NY, USA: Cambridge University Press, 2010.

[37] P. Zhao, G. Fodor, G. Dán, and M. Telek, "A game theoretic approach to setting the pilot power ratio in multi-user MIMO systems," *IEEE Trans. Commun.*, vol. 66, no. 3, pp. 999–1012, 2018.